Quaternary Science Advances 13 (2024) 100122

Contents lists available at ScienceDirect

Quaternary Science Advances

journal homepage: www.sciencedirect.com/journal/quaternary-science-advances

Palaeoenvironmental and chronological context of hominin occupations of the Armenian Highlands during MIS 3: Evidence from Ararat-1 cave

Jennifer E. Sherriff [a,*], Artur Petrosyan [b], Dominik Rogall [c], David Nora [c], Ellery Frahm [d], Tobias Lauer [e,f], Theodoros Karambaglidis [c,g], Monika V. Knul [h], Delphine Vettese [i,j,k], Dmitri Arakelyan [l], Shira Gur-Arieh [m,n], Paloma Vidal-Matutano [o], Jacob Morales [p], Helen Fewlass [e], Simon P.E. Blockley [q], Rhys Timms [q,r], Ani Adigyozalyan [b], Hayk Haydosyan [b], Phil Glauberman [b,s,t], Boris Gasparyan [b], Ariel Malinsky-Buller [c]

[a] Department of Geography, School of Global Affairs, Faculty of Social Science and Public Policy King's College London, UK
[b] Institute of Archaeology and Ethnography, National Academy of Sciences of the Republic of Armenia, Yerevan, Armenia
[c] The Institute of Archaeology, The Hebrew University of Jerusalem, Mt. Scopus, 91905, Jerusalem, Israel
[d] Department of Anthropology, Yale University, New Haven, CT, USA
[e] Max Planck Institute for Evolutionary Anthropology – Department of Human Evolution, Leipzig, Germany
[f] Terrestrial Sedimentology Research Group, Eberhard Karls University of Tübingen, Germany
[g] Department of Geological and Mining Engineering, University of Castilla-La Mancha, Toledo, Spain
[h] Department of Archaeology, Anthropology and Geography, University of Winchester, Winchester, UK
[i] Histoire Naturelle de L'Homme Préhistorique (HNHP, UMR 7194), Muséum National D'Histoire Naturelle (MNHN), Homme et Environnement, Equipe Nomade, CNRS, Institut de Paléontologie Humaine, Sorbonne Universités, Paris, France
[j] Dipartimento Degli Studi Umanistici, Sezione di Scienze Preistoriche e Antropologiche, Università Degli Studi di Ferrara, Ferrara, Italy
[k] Grupo de I+D+i EVOADAPTA (Evolución Humana y Adaptaciones Económicas y Ecológicas durante La Prehistoria), Dpto. Ciencias Históricas, Universidad de Cantabria, Santander, Spain
[l] Institute of Geological Sciences of the National Academy of Sciences of the National Academy of Sciences of the Republic of Armenia, Yerevan, Armenia
[m] Institute for Pre- and Protohistoric Archaeology and Archaeology of the Roman Provinces, Ludwig Maximilian University Munich, Munich, Germany
[n] The Leon Recanati Institute for Maritime Studies, Haifa University, Israel
[o] Departamento de Geografía e Historia, Universidad de La Laguna, San Cristóbal de La Laguna, Spain
[p] TARHA Research Group, Department of Historical Sciences, University of Las Palmas de Gran Canaria, Las Palmas, Spain
[q] Centre for Quaternary Research, Department of Geography, Royal Holloway, University of London, Egham, Surrey, UK
[r] School of Archaeology, Geography and Environmental Science, University of Reading, UK
[s] The Catalan Institute of Human Paleoecology and Social Evolution (IPHES) and Universitat Rovirai I Virgili, Tarragona, Spain
[t] Department of Early Prehistory and Quaternary Ecology, University of Tübingen, Tübingen, Germany

ARTICLE INFO

Keywords:
Middle Palaeolithic
MIS 3
Geoarchaeology
Geochronology
Faunal analysis
Armenia

ABSTRACT

Archaeological and palaeoenvironmental evidence from the Armenian Highlands and wider southern Caucasus region emphasises the significance of Marine Oxygen Isotope Stage 3 (c. 57–29 ka) as a crucial period for understanding hominin behaviours amidst environmental fluctuations. Ararat-1 cave, situated in the Ararat Depression, Republic of Armenia, presents potential for resolving emerging key debates regarding hominin land use adaptations during this interval, due to its well-preserved lithic artefacts and faunal assemblages. We present the first results of combined sedimentological, geochronological (luminescence and radiocarbon), archaeological and palaeoecological (macrofauna, microfauna and microcharcoal) study of the Ararat-1 sequence. We demonstrate sediment accumulation occurred between 52 and 35 ka and was caused by a combination of aeolian activity, cave rockfall and water action. Whilst the upper strata of the Ararat-1 sequence experienced post-depositional disturbance due to faunal and anthropogenic processes, the lower strata remain relatively undisturbed. We suggest that during a stable period within MIS 3, Ararat-1 was inhabited by Middle Palaeolithic hominins amidst a mosaic of semi-arid shrub, grassland, and temperate woodland ecosystems. These hominins utilised local and distant toolstone raw materials, indicating their ability to adapt to diverse ecological and elevation gradients. Through comparison of Ararat-1 with other sequences in the region, we highlight the spatial

* Corresponding author.
E-mail address: jennifer.sherriff@kcl.ac.uk (J.E. Sherriff).

https://doi.org/10.1016/j.qsa.2023.100122
Received 5 June 2023; Received in revised form 9 August 2023; Accepted 13 September 2023
Available online 19 September 2023

variability of MIS 3 environments and its on hominin land use adaptations. This demonstrates the importance of the Armenian Highlands for understanding regional MP settlement dynamics during a critical period of hominin dispersals and evolution.

1. Introduction

Marine Oxygen Isotope stage 3 (MIS 3, c. 57–29 ka; Lisiecki and Raymo, 2005) is a key interval for understanding recent hominin dispersals in Eurasia. This period coincides with the Middle to Upper Palaeolithic 'transition', commonly associated with the spread of anatomically modern humans into Eurasia (Mellars, 2004; Higham et al., 2014; Hublin et al., 2020) and is characterised by sub-orbital scale climatic variability and associated palaeoenvironmental change (Siddall et al., 2008; Van Meerbeeck et al., 2011; Rasmussen et al., 2014). Emerging evidence from regions such as the Levant (Hovers and Belfer-Cohen, 2013; Goder-Goldberger et al., 2020), southeast Europe (Fewlass et al., 2020; Hajdinjak et al., 2021; Hublin et al., 2020; Pederzani et al., 2021; Chu et al., 2022), and southern Europe (Badino et al., 2020; Slimak et al., 2022; Marín-Arroyo et al., 2023) suggest that variable climates and mosaic biomes were key factors in regional hominin adaptions during this period. This emerging perspective highlights the importance of the intricate interactions between hominins and local environmental conditions during this interval. However, regions such as the Armenian Highlands have remained comparatively understudied despite the fact the region has a rich Late Pleistocene archaeological record and is characterised by strong topographic, hydroclimatic and ecological gradients that would have likely amplified environmental changes during intervals of global climatic variability.

A growing number of open-air and cave sites in the Armenian Highlands and southern Caucasus (*sensu* Bailey, 1989) that contain either Middle Palaeolithic (MP) or Upper Palaeolithic (UP) lithic industries correlated to MIS 3 have been subject to detailed geoarchaeological and chronological investigations (see Moncel et al., 2015; Gasparyan and Glauberman, 2022 for a review). Current evidence from these sites suggests that MP lithic technology may have persisted in the Armenian Highlands up to around 30 ka (Egeland et al., 2016; Sherriff et al., 2019; Glauberman et al., 2020a,b; Malinsky-Buller et al., 2021), and these populations were occupying a diverse range of ecological niches and adapting their land use seasonally (Golovanova and Doronichev, 2003; Adler and Tushabramishvili, 2004; Adler et al., 2006; Moncel et al., 2015; Malinsky-Buller et al., 2021; Gasparyan and Glauberman, 2022). Evidence from the archaeological record appears to suggest that elevation may played a key role in subsistence behaviour, relatively high-altitude sites such as Hovk-1 (2040 m asl; Pinhasi et al., 2008, 2011), and Kalavan-2 (1636 m asl; Malinsky-Buller et al., 2021) occupied infrequently or at low intensities due to harsh winter conditions. Lower elevation sites such as Ortvale Klde (530 m asl), appear to be occupied more intensively due to the seasonal availability of migratory herds of prey (Adler et al., 2006). However, a growing number of high elevation sequences (e.g., Colonge et al., 2013; Gasparyan et al., 2014; Malinsky-Buller et al., 2021) do preserve archaeological evidence for more intensive occupations, leading some authors to suggest that elevation is unlikely to be the singular control on occupation intensity (Gasparyan and Glauberman, 2022). Rather, utilisation of local ecological niches and toolstone raw material sources were possibly more important factors in shaping subsistence and land use behaviours during MIS 3.

These adaptions occurred against the backdrop of climatic instability during MIS 3 as revealed by regional palaeoclimatic records. These are principally based on pollen and geochemical evidence from the long lacustrine sequence of Lake Van. These records show that the generally arid conditions of MIS 3 were punctuated by short-lived phases of warmer/more humid conditions, resulting in vegetation fluctuating between non-arboreal dwarf-shrub steppe and desert-steppe communities, and enhanced arboreal vegetation dominated by oak steppe-forest (Litt et al., 2014; Stockhecke et al., 2016; Randlett et al., 2017) Ecological reconstructions from archaeological and sediment sequences across the region hint at complexity in local environmental conditions during MIS 3. Several sequences preserve evidence for relatively stable conditions during the interval (Kandel et al., 2017; Malinsky-Buller et al., 2021; Richter et al., 2020), while others show evidence for fluctuations in arid-humid conditions that may align with regional palaeoclimatic records (Pinhasi et al., 2011; Glauberman et al., 2020a). Elucidating the complex interplay between the environmental change during MIS 3 and its effects on MP hunter-gatherer populations in the Armenian Highlands, however, requires the systematic study of archaeological remains and palaeoenvironmental evidence from sequences that lie across the spectrum of altitudinal gradients and ecological niches observed in the region.

One such site is Ararat-1 cave, which lies at an elevation of 1034 m asl on the eastern flanks of the Ararat Depression in central Armenia. The site preserves stratified lithic artefact and faunal assemblages, making it ideal to investigate local environmental conditions and hominin behaviours in the region. Here we present the first results from the systematic excavation of the cave sediments. Through the application of sedimentological and chronological (luminescence and radiocarbon) techniques which underpin the lithic artefact and faunal evidence, we present; 1) a reconstruction of the depositional history of Ararat-1 cave, 2) an assessment of the integrity of the Ararat-1 artefact assemblage and chronological framework, and 3) a synthesis of palaeoenvironmental conditions at Ararat-1 and the surrounding environment during MIS 3. Through the comparison of the Ararat-1 environmental and archaeological records to other late MP sites, we provide new insights into environmental conditions and hominin behaviours during MIS 3.

2. Site context

Ararat-1 cave (39° 51′ 3.7908″ N, 44° 46' 8.6232" E, 1034 m asl) is situated 2 km east of the town of Ararat on the northeast margins of the Ararat Depression. The cave is a sub-horizontal passage with a maximum known length of c. 6 m, a width ranging from 4 m at the entrance to 1 m at the back of the cave, and a height of c. 4 m from the 2019 cave surface. Whilst the cave systems in this area have yet to be systematically mapped, it has been suggested that Ararat-1 forms part of a more extensive karstic system that extends along the northeastern margin of the Ararat Depression.

The Ararat Depression is an intermontane basin formed as a consequence of the collision between the Eurasian and Arabian tectonic plates from the Miocene onwards (Sosson et al., 2010; Avagyan et al., 2018). The basin occupies an area of c. 1, 300 km^2, and is divided by the Araxes River, which flows in a NW-SE direction through the basin and forms the current border between Armenia (to the north and northeast) and Turkey (to the south and southwest). The north and northeast sector of the Ararat Depression is bounded by the Aragats and Gegham volcanic complexes, both of which were active throughout the Quaternary period (Arutyunyan et al., 2007; Lebedev et al., 2013; Sherriff et al., 2019; Gevorgyan et al., 2020). Mt. Ararat (Masis, Ağri Dağı) stratovolcano (5185 m asl) and associated volcanic complexes lie to the south. The geology of the northeastern sector of the basin is shown in Fig. 1. The northeastern flank of the Depression is steep-sided and formed of Paleogene-Devonian limestones, shales and quartzites which form the Urts Anticline. Quaternary alluvial deposits are found at the base of the flanks; these extend southwest as fan formations towards the centre of

the basin (Avagyan et al., 2018). The basin itself is formed of Cenozoic interbedded clays, gravels, sands, and lava which are capped by recent alluvial deposits formed by the Araks river.

Presently, the area is characterised by a semi-arid climate regime, with temperatures ranging from −5 °C (winter) to + 30 °C (summer) and mean annual precipitation in the range of 300–400 mm (Volodicheva, 2002). Vegetation is dominated by semi-desert and steppe communities, with temperate forest occurring locally in the higher elevation area of the Urts anticline (Volodicheva, 2002). The Ararat Depression has a long history of archaeological investigations, focused principally on the Neolithic sites located in the centre of the basin (Martirosyan-Olshansky et al., 2013; Petrosyan et al., 2014; Badalyan and Harutyunyan, 2014). Several Palaeolithic sites have also been identified on the flanks of the Ararat Depression. These include the sequences of Aghavnatun-1 and Dalarik-1, both of which have yielded Lower Palaeolithic lithic artefact assemblages (Gasparyan et al., 2014; Gasparyan et al., 2014)., The open-air site of Barozh-12, located on the northwestern margins of the Ararat Depression has been systematically excavated by Glauberman et al. (2020a, b). The site has yielded a high-density late MP obsidian artefact assemblage recovered from an alluvial-colluvial sequence dated to 60.2 ± 5.7 to 31.3 ± 4 ka.

3. Methods

3.1. Field methods

In 2019, a 1 m^2 grid was established using a Leica FlexLine TS07 total station covering the cave platform and interior. This allowed for the 3D recording of sample locations, sedimentary units, and archaeological and macrofaunal remains by associating a local coordinate system and datum with the grid. A 10 m^2 area in the northwest sector of the cave (grid squares J11–14, K11–13, L11-13) was selected for excavation during this season (Fig. 2). Each 1 m^2 square was excavated by hand in 50 mm thick 'spits' resulting in a trench excavated to a depth of c. 2 m. Faunal remains and lithic material larger than 20 mm were recorded with respect to the local grid coordinates and datum. All excavated sediment was dry sieved on-site using 5 mm mesh and material recovered in the coarse fraction (i.e., larger than 5 mm) was retained for analysis. A c. 10% sub-sample of material excavated from square K12 was retained for floatation, in total 12 samples were analysed.

The north and west sections of the exposed trench were drawn and described following standard protocols (Fig. 2). 2 cm thick blocks of sediment were sampled contiguously through the trench for laboratory analysis. 4 undisturbed blocks of sediment were sampled for micromorphological analysis from Units 2a, 2 b, 2 d, and 3. Due to the unconsolidated nature of the sediments, sampling had to be adapted on-

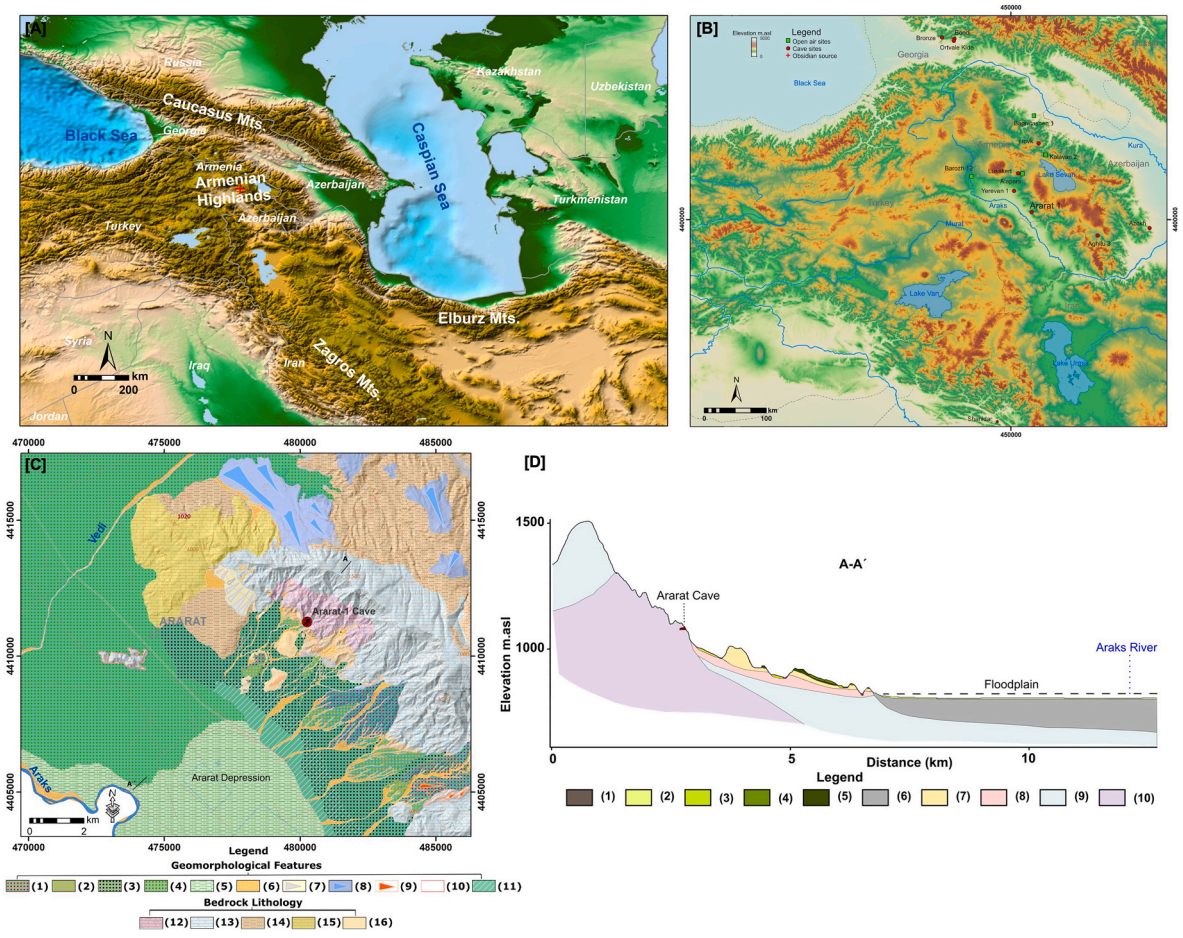

Fig. 1. A) Location of the Armenian Highlands. B) Location of Ararat-1 and Middle Palaeolithic archaeological sequences. C). Simplified geological map showing Ararat-1. Legend: 1) alluvial fan 1, 2) alluvial fan 2, 3) alluvial fan 3, 4) alluvial fan 4, 5) Araxes River floodplain, 6) active channels, 7) debris flow, 8) carbonate slope sediments, 9) pediment, 10) inselberg island, 11) intensive anthropic use, 12) Devonian limestones and sandstones, 13) Carboniferous limestones and sandy shales, 14) Paleogene limestones, sandy limestones, siltstones, conglomerates and clays, 15) Lower Oligocene volcaniclastic and 16) Neogene limestones. D) Geological cross-section of the Ararat - 1 locale. Legend: 1) active channels, 2) Araxes river floodplain, 3) alluvial fan 3, 4) alluvial fan 2, 5) alluvial fan 1, 6) Ararat basin Plio-Quaternary sequence comprisgin fluvial, lacustrine, and volcanic deposits, 7) Lower Oligocene volcaniclastic, 8) Paleogene limestones, sandy limestones, siltstones, conglomerates and clays, 9) Carboniferous limestones and sandy shales and 10) Devonian limestones and sandstones.

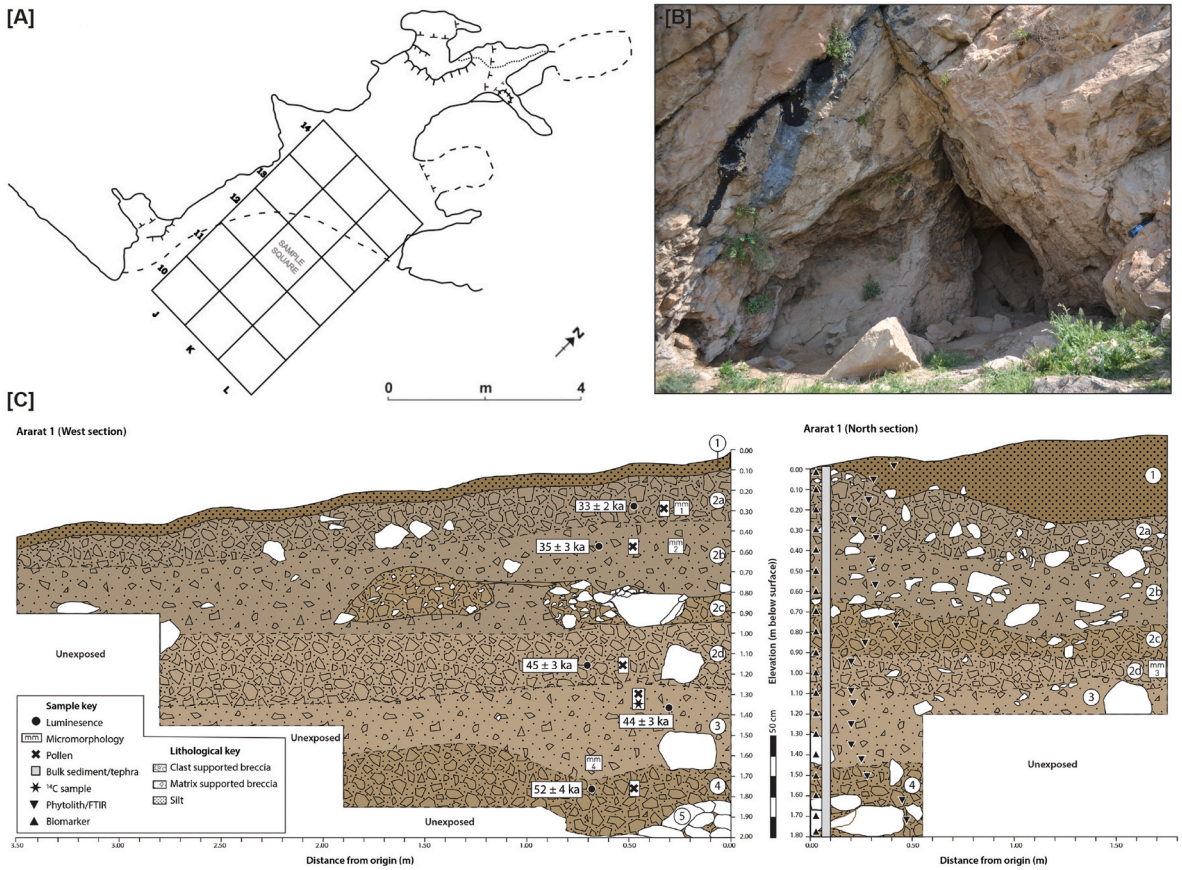

Fig. 2. Summary of Ararat-1 exacavations. (A) Plan sketch of the cave showing the position of 2019 excavation grid squares. (B) Photograph showing Ararat-1 cave entrance. (C) Section drawings showing the main stratigraphic units and sample locations.

site. Samples from Units 2a and 2 b were sampled using 10 × 6 cm stainless steel Kubiena tins, whilst Units 2 d and 3 were sampled through the extraction of 10 × 10 cm blocks using plaster of Paris. Five sediment samples were collected from Units 2a-3 for pIR225 dating using opaque stainless-steel tubes hammered horizontally into the west section face (Fig. 2).

3.2. Sedimentology

Prior to laboratory sedimentological and geochemical analyses, contiguous 2 cm samples were combined to create 4 cm sub-samples. The resulting 45 samples were then oven dried at 40 °C and disaggregated using a pestle and mortar. Dried samples were placed through a 2 mm mesh, and < 2 mm sub-samples were retained for sedimentological and geochemical analyses. Mass-specific magnetic susceptibility was measured using a Bartington MS2 meter with MS2c dual frequency sensor at low (0.46 kHz, χ^{lf}) frequency, following the protocol outlined in Dearing (1999). Percentage organic content was estimated from loss-on-ignition at 550 °C (Heiri et al., 2001), and the percentage calcium carbonate equivalent was determined using a Bascomb Calcimeter. Particle size analysis was undertaken using a Malvern Mastersizer 3000 laser granulometer with a Hydro UM accessory following the protocol described in Glauberman et al. (2020a). Micromorphology samples were prepared using standard impregnation techniques developed in the Centre for Micromorphology at Royal Holloway, University of London. Thin sections were analysed using an Olympus BX-50 microscope with magnifications from 20× to 200x and photomicrographs were captured with a Pixera Penguin 600es camera. Thin section description followed terminology adapted from Bullock et al. (1985) and Stoops et al. (2018).

3.3. Chronology

3.3.1. Luminescence dating

Luminescence measurements were undertaken using the pIR225 approach as applied at several other Late Pleistocene sequences in Armenia (Glauberman et al., 2020a; Malinsky-Buller, et al., 2021). Given the high aeolian inputs into the cave, the 4–11 μm polymineral fine-grain fraction was selected for analysis, with the equivalent dose (De) rate estimated through the pIR225 approach adapted from Malinsky-Buller et al. (2021). The method is described in full in supplementary information 1. Dosimetry data, equivalent doses and luminescence age estimates are presented in Table 3.

3.3.2. Radiocarbon dating

Six charcoal samples and nine animal bones from units 2a-b, 2 d, 4 and 5 were selected from the excavated material for accelerator mass spectrometer (AMS) dating (Table 4). A full description of the methods is provided in supplementary information 1. In summary, charcoal samples were pre-treated with the acid-base-acid (ABA) protocol outlined in Dee et al. (2020) and dated at the Centre for Isotope Research (CIO) at the Energy and Sustainability Research Institute (ESRIG) of the University of Groningen, (lab code GrM). Collagen extraction of bone material was undertaken at the Max Planck Institute for Evolutionary Anthropology using the ABA plus ultrafiltration protocol described in Fewlass et al. (2019) and Talamo et al. (2021) Eight of the bones failed to yield any collagen and only one bone had a collagen yield of 8.5%, with elemental (C%, N%, C:N) and stable isotopic values ($\delta^{13}C$ and $\delta^{15}N$) falling within established ranges of well-preserved collagen (van Klinken, 1999) (SI 1, Table 1). The collagen extract was AMS dated at the Klaus-Tschira-AMS facility in Mannheim (MAMS).

Table 1
Description and interpretation of sedimentological units in Ararat-1.

Unit	Depth (m below datum)	Description	Preliminary interpretation
1	0.0–0.02	Massive fine-medium silt with isolated coarse sand – granule-sized subangular grains. Modern plant and organic material frequent. 10YR/5/4. Sharp-diffuse contact with:	Modern cave material – dung and grass.
2a	0.02–0.40	Massive moderately-poorly sorted, matrix supported, fine-medium silt. Clasts range in size from granules-fine pebbles, angular to very angular, limestone, carbonate coated. No visible orientation. Modern root growth throughout. 10YR/6/3. Diffuse contact with:	Aeolian with larger clasts representing rockfall from cave interior.
2b	0.40–0.75	Massive, poorly sorted, matrix supported fine-medium silt with clasts (not as common as 2a). Clasts range in size from small pebbles-cobbles, angular-very angular, limestone, carbonate coated. Several clasts are orientated towards cave entrance. Rare sub-rounded clasts. 10YR/6/3. Diffuse contact with:	
2c	0.75–0.94	Massive, poorly sorted clast rich fine-medium silt with clasts. Clasts appear as a discontinuous band across the section face, range in size from small-pebbles-large cobbles, angular-very angular, limestone, carbonate coating. 10 YR 6/3. Diffuse contact with:	Aeolian. Large clasts represent rockfall from cave roof collapse. Much higher energy event than those above/below.
2d	0.94–1.22	Massive, poorly sorted matrix rich fine-medium silt with clasts. Clasts range in size from medium pebbles-boulders (boulders rare), subangular-very angular, limestone, carbonate coated. 10YR/6/3. Diffuse contact with:	Aeolian with larger clasts representing rock fall from cave interior.
3	1.22–1.41	Massive, moderately sorted fine-medium silt with clasts. Clasts range in size from small pebbles-boulders, angular-very angular, limestone, carbonate coated. High angle of dip in some of the clasts. 10YR/6/3. Matrix forms very weakly developed cm-scale aggregates, with sand grains and rare powdery carbonate. Rare Fe/Mn staining. Diffuse contact with:	Altered aeolian sediments with large clasts representing rock fall. Alteration of aeolian sediments may be related to incipient soil formation/inwashing of material/cementation from dripline waters.
4	1.41–1.83	As [2 d]	
5	Base of trench	Base of unit not reached.Massive moderately-poorly sorted, matrix supported fine-medium silt with clasts. Clasts range in size from granules-fine pebbles, angular to very angular, limestone, carbonate coated. 10YR/6/4 (wet).	Aeolian with larger clasts representing rockfall from cave interior [?]

Table 2
Summary of micromorphological features in Ararat-1.
>70% - very abundant, 50–70% - abundant, 30–50% - common, 15–30% - frequent, 5–15% - few, <5% - rare, trace – single occurrence on a slide c/f ratio = 10 μm.

Code	Unit	Depth (m below datum)	Fabric & Structure	Features & Inclusions
ARA19 MM-1	2a	0.3–0.4	Brown-yellow (PPL) sandy silt loam. Poorly sorted. Massive. Single-spaced porphyric to chitonic distribution. 50% porosity. Common sub horizontal planar voids at base of slide. Common vughs throughout. Platy-vughy structure. Micritic- microspartic calcite and organoclastic groundmass. Crystallitic b-fabric. c/f ratio; 70:30.	Abundant angular-subangular coarse silt-pebble size spartic limestone with rare peculiar alteration to clay. Frequent quartz/feldspar medium silt grains. Trace volcanic ash, basaltic lithic, siltstone, and indet. metamorphic grains. Few lithoclasts of tufa and banded speleothem. Rare rounded pedorelicts. Few bone fragments. Few charcoal fragments, mainly amorphous, but occasional fragments retain plant tissue structure. Rare orthic Fe/Mn nodules in upper part of slide.
ARA19 MM-2	2 b	0.4–0.5	Brown-yellow (PPL) sandy silt loam. Poorly sorted. Massive. Single-spaced porphyric to chitonic distribution. 5% porosity. Vughs. Massive -weakly vughy microstructure. Micritic- microspartic calcite and clastic groundmass. Crystallitic - speckled b-fabric. c/f ratio; 80:20.	Abundant angular-subangular coarse silt-pebble spartic limestone with rare micritic calcite-clay continuous coatings. Frequent quartz/feldspar medium siltgrains. Trace volcanic ash and pumic lapilli. Rare lithoclasts of tufa and banded speleothem. Rare rounded pedorelicts. Rare bone fragments. Few amorphous charcoal fragments. Common black-brown amorphous organic residues. Rare phosphatic nodules with black amorphous organic inclusions. Few zones of calcite depletion of groundmass.
ARA19 MM-3	2 d	1.0–1.1	Brown-yellow (PPL) sandy silt loam. Poorly sorted. Massive. Single-spaced porphyric to chitonic distribution. 10% porosity. Vughs and straight planar voids. Massive -weakly vughy microstructure. Micritic-microspartic calcite and clastic groundmass. Crystallitic - speckled b-fabric. c/f ratio; 60:40.	Frequent angular-subangular coarse silt-pebble spartic limestone with rare micritic calcite-clay continuous coatings and trace micritic calcite-clay capping of grains. Frequent quartz/feldspar medium silt grains. Rare rounded pedorelicts. Rare bone fragments. Few amorphous charcoal fragments. Common black-brown amorphous organic residues. Rare plant tissue remains with groundmass infillings. Rare sub-vertical passage features. Few zones of calcite depletion of groundmass.
ARA19 MM-4	3	1.5–1.6	Brown-yellow (PPL) sandy silt loam. Poorly sorted. Massive. Single-spaced porphyric. 40% porosity. Abundant vughs and straight planar voids. Vugh microstructure. Micritic- microspartic calcite and organoclastic groundmass. Crystallitic - speckled b-fabric. c/f ratio; 80:20.	Common angular-subangular medium silt- pebble spartic limestone with rare micritic calcite-clay continuous coatings, trace micritic calcite and silt discontinuous coatings and trace continuous phosphatic continuous coating. Frequent quartz/feldspar medium silt grains. Rare volcanic ash and basaltic lithic fragments. Rare lithoclasts of tufa and banded speleothem. Rare rounded pedorelicts. Few bone fragments with trace evidence of micritisation. Rare phosphatic nodules with black amorphous organic inclusions. Few amorphous charcoal fragments and rare indet. plant tissue residues. Rare euhedral spar calcite coating around voids.

Table 3
Ararat-1 cave dosimetry data, equivalent doses (mean values with standard error) and luminescence age estimates.

Sample Code	Unit	Sample ID (L-Eva)	U (ppm)	Th (ppm)	K (%)	Total doserate (mGy/a)	De pIRIR225 (Gy)	pIRIR225 age (ka)
OSL 1	2a	2037	2.5 ± 0.3	4.4 ± 0.3	1.17 ± 0.13	2.42 ± 0.18	80.8 ± 0.5	33.4 ± 2.5
OSL 2	2 b	2038	2.6 ± 0.3	4.4 ± 0.3	1.22 ± 0.13	2.50 ± 0.18	87.8 ± 0.5	35.1 ± 2.5
OSL 3	2 d	2039	2.2 ± 0.3	4.7 ± 0.3	1.30 ± 0.08	2.48 ± 0.16	112.0 ± 0.9	45.1 ± 3.0
OSL 4	3	2040	2.4 ± 0.3	5.0 ± 0.4	1.38 ± 0.10	2.64 ± 0.17	117.0 ± 1.1	44.3 ± 2.9
OSL 5	4	2041	2.0 ± 0.3	4.9 ± 0.3	1.42 ± 0.12	2.52 ± 0.17	132.0 ± 0.6	52.4 ± 3.6

3.4. Faunal remains

Macrofaunal remains recovered from the sequence were studied at the University of Ferrara and the MONREPOS archaeological research centre. Taxonomic classification was aided by anatomical atlases and comparative collections where necessary. Taphonomic alteration of the material was recorded using a combination of the naked eye and low-powered microscopy and classified using established protocols (Behrensmeyer, 1978; Binford, 1981; Blumenschine et al., 1996; Fernández-Jalvo and Andrews, 2016; Vettese et al., 2020). Special attention was given to possible anthropogenic modification, with burn damage and cutmarks described following the criteria of Stiner et al. (1995) and Lyman (2008) respectively.

Microfaunal remains were studied at the University of Winchester and the Catalan Institute of Human Palaeoecology and Social Evolution (IPHES). Identification was aided through the use of a Zeiss SteREO Discovery V8 (0.63x to 10x magnification) stereomicroscope, a digital camera (5 megapixels) with colour-CMOS-sensor, and a Zeiss Smartzoom 5 (34x to 1010x magnification) 3D digital microscope. Taphonomic alteration of the remains was classified following the criteria of Lyman (2008) and Fernández-Jalvo and Andrews (2016). Macrofauna counts are presented as the number of remains (NR) number of identified species (NISP) and the minimum number of individuals (MNI). Microfaunal counts are presented as NISP and NR.

3.5. Charcoal remains

Charcoal remains were mostly recovered through flotation, while 21 fragments were handpicked from the wet sieving residue. Each charcoal fragment was fractured manually to provide transverse, tangential, and radial sections for taxonomic identification using a Nikon Labophot-2 bright/dark field incident light microscope with 50–500 × magnification at the University of Las Palmas de Gran Canaria. Botanical identification was performed using specialised plant anatomy atlases (Fahn et al., 1986; Parsapajouh et al., 1987; Schweingrüber, 1976, 1990) and online databases (Inside Wood, 2004), in addition to a reference collection of modern charred woody taxa. All the available charcoal samples were analysed. Photography and detailed observations of the anatomical and taphonomic features were carried out using a Zeiss EVO MA 15 scanning electron microscope (SEM) at the General Research Support Service (SEGAI), University of La Laguna.

3.6. Artefacts

This study includes a general description of the artefact assemblage recovered from Ararat-1 to assess stratigraphic patterning. The recovered lithics were inventoried at the Institute of Archaeology and Ethnography of the National Academy of Sciences, Republic of Armenia (IAE NAS) according to size (<10 mm and >10 mm), raw material, and class and technological categories. Results of a detailed attribute analysis of each artefact following the protocol outlined in Hovers (2009) and Malinsky-Buller et al., 2021 are forthcoming in a separate study. In addition to the lithic assemblage, ceramic fragments were also recovered from the Ararat-1 sequence. These fragments were studied at the IAE NAS, where each fragment was assigned a class and archaeological designation.

4. Results

4.1. Stratigraphy, sedimentology & micromorphology

Field sedimentological descriptions for the north and west profiles of the Ararat-1 trench are presented in Table 1 and section drawings are shown in Fig. 2. The strata exposed during the 2019 excavation (Units 1, 2a-d, 3, 4, 5) are comprised principally of matrix to clast supported angular to very angular limestone pebbles to cobbles in a fine-medium silt matrix. Carbonate coatings on clasts are common throughout the sequence. Units 1–5 are differentiated based on the size and frequency of gravel clasts and concretionary fabrics.

Unit 5 is represented at the base of the sequence and the lowermost contact of this unit was not reached during the 2019 excavation. The unit comprises matrix-supported angular to very angular limestone clasts in a matrix of fine silt to clay. Unit 4 is characterised by massive, poorly sorted clast-rich angular to very angular limestone pebbles to cobbles in a fine-medium silt matrix. Overlying this, Unit 3 is formed of massive, moderately-poorly sorted, matrix-supported, angular to very angular limestone pebbles to cobbles in a matrix of fine-medium silt. The matrix is carbonate-bonded and ferruginous mottling is present. Unit 2 d has comparable properties to Unit 4, whilst Unit 2c is comprised of massive, poorly sorted clast-rich angular to very angular limestone clasts in a fine-medium silt matrix. Clasts range in size from small pebbles to large cobbles. Units 2 b-a are formed of massive moderately-poorly sorted matrix supported angular to very angular limestone clasts in a matrix of fine-medium silt. Unit 2 b is generally more clast rich than 2a and the clast size is larger (2a: granules-fine pebbles, 2 b: fine pebbles-cobbles). The uppermost unit (Unit 1) comprises massive humic fine-medium silt representing the modern cave floor.

Fig. 3 presents the results of the bulk sedimentological analysis through the Ararat-1 sequence. Broadly, the sequence is characterised by low organic content (1. −9.8%), low χ^{lf} (12.3–17.7 10^{-8} m^3 kg^{-1}) and relatively high $CaCO_3$ values (27.7–48.2%). Whilst there are no substantial variations in $CaCO_3$ content among strata, differences occur in both magnetic susceptibility and organic content. χ^{lf} values show a broad difference between the upper and lower strata, where mean χ^{lf} values in Units 5–3 are 14.9 10^{-8} m^3 kg^{-1}. These values decrease through Unit 2 d to 12.3 10^{-8} m^3 kg^{-1}, above which they increase to 15.9 10^{-8} m^3 kg^{-1}in Units 2c-2b. Unit 2a is characterised by relatively high mean χ^{lf} values of 17.0 10^{-8} m^3 kg^{-1}. Organic content shows a slightly different trend, with relatively lower values through Units 4–3 (mean = 3.2%), before increasing through Unit 2 d to values of c. 5%. A mean value of 5.1% characterises Units 2a-2c. Unit 1, representing the modern cave floor is characterised by lower χ^{lf} (14.6 10^{-8} m^3 kg^{-1}) and $CaCO_3$ (38.7%), and elevated organic content (9.8%) in comparison to the underlying units.

The particle size distribution of the <2 mm fraction indicates that Ararat-1 sediments are poorly sorted (σ_G 3.2–5.7), with a coarse silt-fine sand texture. Median particle size through the sequence range between 38 and 75 μm. There is minimal variation in particle size through Units 2a-3, however, Unit 4 is characterised by a relatively higher proportion of clay relative to the overlying strata (Fig. 4). Whilst the deposits are poorly sorted, and polymodal in their particle size distribution, it is interesting to note that modal particle sizes are consistent throughout the sequence, with the first modal grain size value falling in the range of

Table 4
AMS radiocarbon dating of the Ararat-1 cave material. Calibration was carried out using the IntCal20 calibration curve (Reimer et al., 2020) in OxCal 4.4 (Bronk-Ramsey, 2009). Also presented are the location of the bone samples which yielded low collagen yields (<1%).

Sample elevation (cm below datum)	Unit	Square	Sample material	Collagen yield (%)	$\delta^{13}C$ (‰)	$\delta^{15}N$ (‰)	%C	%N	C: N	Lab code[a]	$F^{14}C$	±1σ	^{14}C age (BP)	±1σ	Calibrated range 68.3%	Calibrated range 95.4%
41	2a	J13	Charcoal		−27.01		60.8			GrM-23371	1.3305	0.0029	(>AD 1950)		modern	modern
41	2a	J13	Charcoal		−25.78		62.7			GrM-23370	0.9569	0.0025	354	21	cal AD 1480 –1623	cal AD1462–1634
52	2 b	J13	Bone	8.5	−18.7	9.3	44.5	16.1	3.2	MAMS-48364			131	20	cal AD 1687–1927	cal AD 1680–1940
54	2 b	J13	Charcoal		−22.95		63.8			GrM-23368	0.9663	0.0023	275	19	cal AD 1529–1656	cal AD 1523–1662
54	2 b	J13	Charcoal		−23.05		58.4			GrM-23369	0.957	0.0026	353	22	cal AD 1480–1623	cal AD 1460–1634
69	2 b	J13	Charcoal		−25.13		60.1			GrM-23367	0.8427	0.0023	1375	22	cal AD 647–664	cal AD607–675
157	3	J13	Charcoal		−24.36		59.4			GrM-23366	0.0069	0.0007	39,950	900	43,990–42,720 cal BP	44,660–42,370 cal BP
Samples with low collagen yields																
	2 b	J12	Bone	0.0						R-EVA 3568						
	2 b	J13	Bone	0.1						R-EVA 3569						
	2 b	L13	Bone	0.0						R-EVA 3567						
	2 b	K13	Bone	0.4						R-EVA 3566						
	2 b	L11	Bone	0.1						R-EVA 3562						
	2 d	K13	Bone	0.1						R-EVA 3565						
	3	K13	Bone	0.0						R-EVA 3564						
	5	L12	Bone	0.0						R-EVA 3563						

[a] Laboratory code given for AMS samples charcoal samples conducted at the Centre for Isotope Research, University of Groningen (GrM) and for bone collagen conducted at Curt-Engelhorn-Centre for Archaeometry Klaus-Tschira-AMS facility (MAMS). Laboratory code for bone sample with no collagen from the Department of Human Evolution, Max Planck Institute for Evolutionary Anthropology (R-EVA).

62–72 μm and the second modal grain size value falling in the range of 12–20 μm.

The main micromorphological properties of the Ararat-1 sediments (Units 3, 2 d, 2 b, 2a) are presented in Table 2 with photomicrographs of key features shown in Fig. 4. The overall microstructure of the sequence is massive to vughy sandy silt loam, with a single-spaced porphyric – chitonic coarse-fine (c/f ratio at 20 μ β-fabric. Evident through the sequence are subtle changes to the microstructure, with Unit 2a exhibiting a platy microstructure (Fig. 4a), with both Units 2a and 3a exhibiting a higher degree of porosity (c. 40–50 % of the slide cover) in comparison to Units 2 b and 2 d (Fig. 4b). Sub-vertical passage features are present in Unit 2 d (Fig. 4c), and zones of calcite depletion within the groundmass occur in both Units 2 b and 2 d (Fig. 5d).

The coarse fraction of the Ararat-1 sediments is dominated by angular to sub-angular spartic limestone clasts, with the presence of rounded pedorelicts, volcanic material (ash and mafic lithic fragments) and carbonate (tufa and speleothem) lithoclasts (Fig. 4e) throughout all units. On occasion, limestone clasts show peculiar alteration to clay (*sensu* Bullock et al., 1985), and some limestone clasts possess continuous clay-micritic calcite coatings (Fig. 4f). These coatings tend to be more frequent in Unit 3, and there is also evidence for calcite-silt clast cappings and phosphatic continuous clast coatings within this Unit. Organic residues occur throughout all units and take form as principally amorphous brown-black organic fragments and angular charcoal fragments. Occasional charcoal fragments preserve plant tissue structure in Unit 2a (Fig. 4g), and plant tissue remains with groundmass infillings are present in Unit 2 d. Bone fragments are present throughout the sequence; they show minimal alteration (although breakage is common), and rarely they show evidence of phosphomicrititisation, with the occurrence of microspartic calcite pendant cements (Fig. 4h). Typic phosphate nodules are identifiable throughout the sequence (Fig. 4i), and rare orthic Fe/Mn nodules are present in Unit 2a and Unit 3. Spartic calcite coatings around voids are also present in Unit 3.

The roughly stratified and poorly sorted nature of the deposits at Ararat-1 is consistent with the deposition of principally clastic sediments near the cave entrance (White, 2007). The angular limestone clasts forming the significant volume of deposits represent the local transport and deposition of material, likely through a combination of 1) debris flows within, or near the entrance to, the cave system, and 2) periodic rockfalls within the cave. The sedimentological properties of the surrounding matrix are consistent with predominantly aeolian sedimentation, with some contribution of material from debris flows. Such an interpretation is supported by the polymodal particle size distribution of the strata, with the finer modal size fraction consistent with the suspension of material by wind action (e.g., Lin et al., 2016). The presence of pedorelicts and fragments of volcanic material at the microscale also indicate inputs of surficial material from the plateau above the cave through the epikarst via water action. Transport of material from elsewhere within the karstic system is also evidenced by the presence of tufa and speleothem lithoclasts (Bosch and White, 2004; Mallol and Goldberg, 2017). $CaCO_3$ values through the Ararat-1 sequence are generally high, reflecting the contributions of the limestone bedrock lithology, secondary carbonates formed within the sequence (carbonate clast coatings), and carbonate derived from aeolian sources. The relatively low χ^{lf} values observable throughout the sequence likely reflect the high abundance of diamagnetic carbonate material in the deposits (Dearing, 1999), but also contributions of other mineralogies with the transport of non-carbonate material into the cave system through aeolian, debris

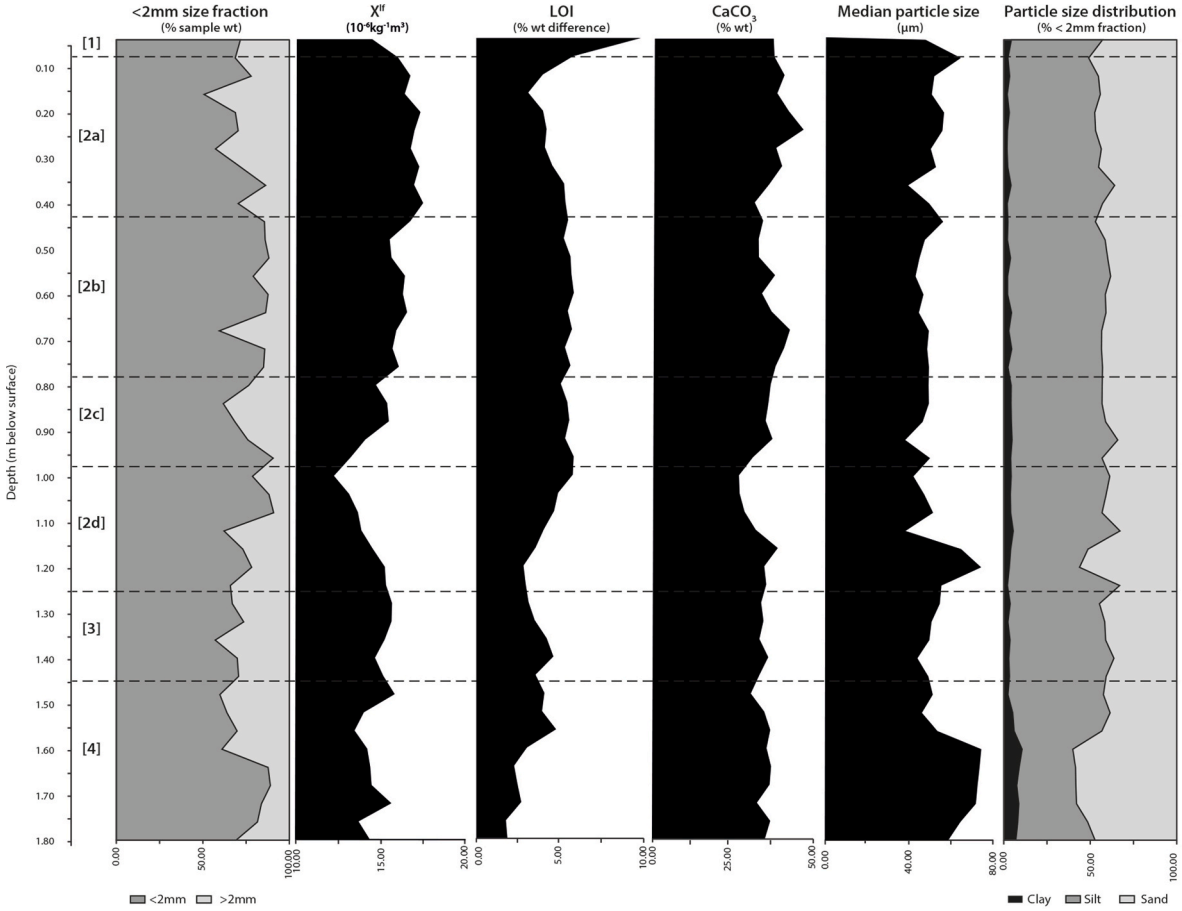

Fig. 3. Summary of bulk sedimentology from Ararat11. Shown are the >2 mm and < 2 mm percentage size fraction, low frequency magnetic susceptibility, LOI, % carbonate content, median particle size (of the < 2 mm fraction) and particle size distribution of the <2 mm size fraction.

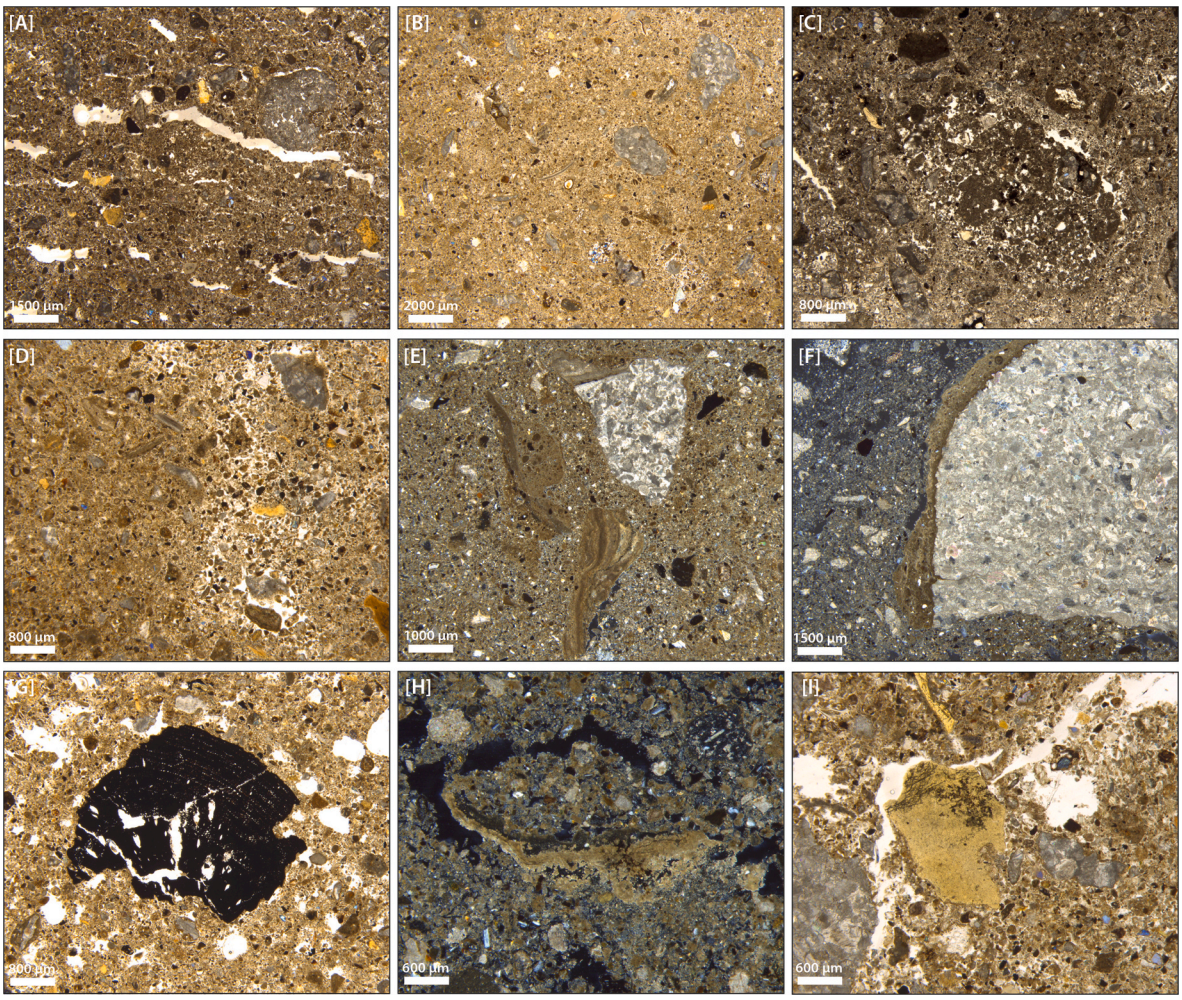

Fig. 4. Photomicrographs of representative micromorphological features in the Ararat 1 sequence. A) platy microstructure (Unit 3a [plane polarised light; PPL]), B) massive microstructure observable in units 2 b, 2 d and 3 (PPL), C) sub-vertical passage feature (Unit 2 d [PPL]), D) zone of calcite depletion (evident in the right of the image, Unit 2 b [PPL]), E) carbonate lithoclasts (Unit 2 b [cross polarised light; XPL], F) spartic clast with clay-calcite coating (Unit 3 [XPL]), G) charcoal fragment with tissue structure preserved (Unit 2a [PPL]), H) bone fragment with phosphomicritic pendant coating (Unit 3 [XPL]), I) typic phosphate nodule (Unit 2 b [PPL]).

flow and infiltration processes. Differences in χ^{lf} values through the sequence are therefore suggested to represent the differing contributions of these non-carbonate mineralogies.

Whilst there is evidence for stratification of the Ararat-1 deposits, broadly there are no large differences in the bulk sedimentological parameters and micromorphological properties between units, suggesting no significant shift in the style of sediment deposition through the sequence. Variations in the frequency and size and clasts between strata are interpreted here to reflect the relative contributions of clastic sediment supply. The clearest example of this is the angular to very angular boulder clasts that characterise Unit 2c. These are interpreted here to represent a rockfall event within the cave system. The discontinuous nature of this unit suggest the rockfall event may have been localised within cave system; however these larger boulders may have acted to shield the lower Ararat-1 strata from further remobilisation and erosion.

There is evidence for syn- and post-depositional modification of the Ararat-1 sediments. This is reflected principally by the presence of secondary carbonate features at both the macroscale (clast coatings) and microscale (clast and void coatings and pendants cements), indicating the dissolution and translocation of calcium down sequence due to water activity (Karkanas and Goldberg, 2010). Calcite depletion features observable in the upper strata and generally higher abundance of secondary carbonate features in Unit 3 support such a hypothesis. The presence of apatite nodules and phosphate cements within the sequence also indicates the translocation of phosphate within the Ararat-1 sequence, through a combination of the dissolution of bone apatite due to weathering processes and phosphate enrichment by animal excretory products (Karkanas and Goldberg, 2010). In both cases, the decay of organic matter/bone led to enhanced phosphate concentrations in water percolating through the Ararat-1 strata, ultimately leading to the *in-situ* formation of phosphate minerals (Shahack-Gross et al., 2004). Post-depositional disturbance of the sequence is also evidenced by the occurrence of passage features indicating bioturbation of the sediments by faunal activity, and the platy microstructure within the upper part of Unit 2a. Such a structure is commonly associated with trampling and compaction of the cave floor by anthropogenic and/or faunal activity (Rentzel et al., 2017). Indeed, the presence of ceramic and modern animal excrement found on the modern cave floor, and the presence of both intrusive ceramics and modern bone material within Units 2a-2c (see sections 4.3 and 4.5 below) supports such an interpretation.

4.2. Chronology

The results of pIR225 luminescence dating of Units 2a - 4 are presented in Table 3. Age estimates place the interval of sediment accumulation in Ararat-1 between 52.4 ± 3.6 ka (Unit 4) and 35.1 ± 2.5 ka

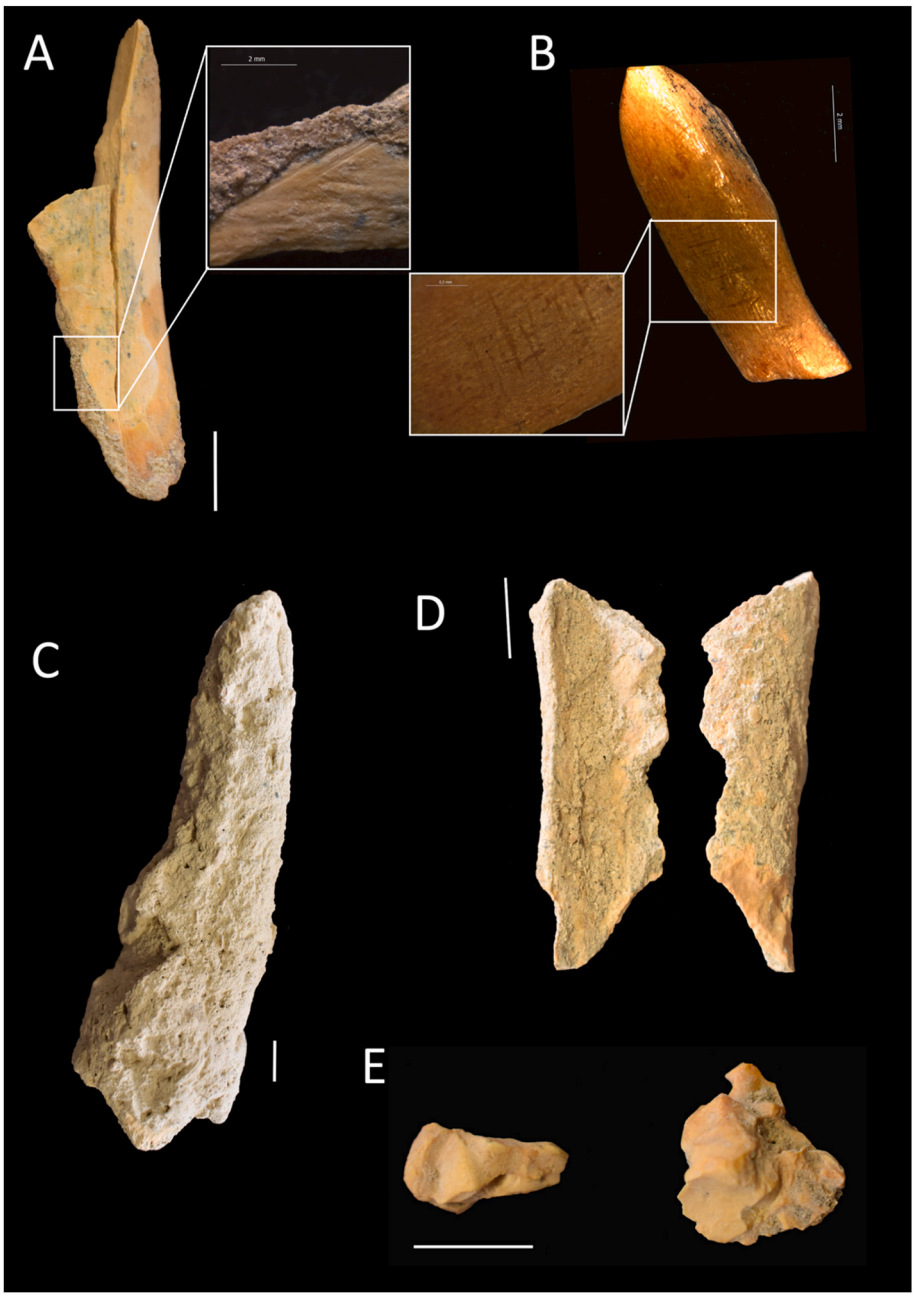

Fig. 5. Examples of taphonomical modifications observed on the bones from Ararat-1. (A) & (B) anthropic modifications, possible cutmarks on undetermined long bones. (C) Horn of Capra sp. With a concretion coating (D) Overlapped and consecutive notches on long bones. (E) Two digested undetermined bones by carnivores. Scale = 1 cm.

(Unit 2a) with no evidence of a considerable temporal hiatus in the accumulation of the fine-grained fraction of Units 4-2a. ^{14}C age estimates for the charcoal fragments and bone remains are presented in Table 4. The single bone fragment from Unit 2 b which preserved a high enough concentration of collagen to produce an age yielded an estimate of cal AD 1680 – 1940 (2σ). Calibrated ^{14}C ages of the charcoal fragments from Units 2a and 2 b range from cal AD 607–675 (2σ) to modern. A single charcoal fragment from Unit 3 has yielded a calibrated age of 44,660–42,370 cal BP (2σ).

The strong De-averaging effect associated with the pIR225 approach means that it is not possible to detect sediment mixing or incomplete bleaching, therefore the obtained overdispersion rate are very low (<3%). Utilisation of the 4–11 μm polymineral fine-grain fraction for analysis means that there is a lower likelihood of incomplete bleaching occurring (Buylaert et al., 2012). Given the evidence for post-depositional disturbance of the sedimentary sequence, it is likely that some sediment mixing has occurred. However, the coherence of calculated pIR225 ages through the sequence suggests that this may have had a limited effect and the calculated pIR225 ages provide suitable first estimates for the timing of sediment accumulation at Ararat-1.

The recent ages of the charcoal fragments and bone from the upper strata of the Ararat-1 cave sequence are clearly at odds with the pIR225 luminescence ages obtained from the same strata which have yielded an age range of 33.4 ± 2.5 ka (Unit 2 b) and 35.1 ± 2.5 ka (Unit 2a) respectively. The elemental and isotopic composition of the single bone fragment with good collagen preservation recovered from Unit 2 b indicates that the younger age estimate of this material is not the outcome of contamination. Instead, it implies the fragment has intruded into the

older sediment. Poor collagen preservation in other bone samples from the sequence also suggests that taphonomic processes affecting the Ararat-1 upper strata may have led to these young ages. This hypothesis is supported by the presence of bioturbation and modern root features, as well as ceramic fragments recovered from Units 2a-2c at a maximum depth of 0.8 m below surface. The presence of refits of medium-sized ungulate bone fragments recovered from Units 2a and 2c suggests that post-depositional translocation of material through the Ararat-1 sedimentary has also taken place. All of these lines of evidence indicate that more recent (Holocene) material has intruded into the Ararat-1 upper strata, and the ^{14}C ages of the charcoal and bone from this part of the sequence reflect this. In contrast, comparable ^{14}C age of the charcoal and pIR225 depositional age estimate of Unit 3 sediments suggest that the lower strata of Ararat-1 were less impacted by post-depositional processes and can provide more reliable ages of deposition at the site.

4.3. Macrofauna & microfauna remains

The Ararat-1 macrofauna assemblage is comprised of 1050 bones and bone fragments (Table 5). These are most abundant in Units 4 (NR = 328), Unit 3 (NR = 252) and Unit 2 d (NR = 298). Units 2a - 2c yielded comparatively fewer remains (NR 2a = 34, 2 b = 26 and 2c = 96). The macrofaunal assemblage is characterised by a high quantity of unidentified bone splinters (NR = 790) and isolated teeth (NR = 69). The majority (69%) of remains are 20 mm or smaller in size. Complete elements are represented by only three isolated teeth, one astragalus, one sesamoid, two long bones (femur and metapodial) and one vertebra. Cortical surfaces are poorly preserved with carbonate concentrations, dissolution and exfoliation observed across the majority of bone surfaces. Throughout the sequence, there is evidence for water dissolution (ranging between 5 and 31% NR in each unit) and root etching (ranging between 16 and 45% NR in each unit). There is limited evidence for cracking, polishing, or blunting of bones, and only one bone fragment (from Unit 2c) shows evidence of rodent marks. Carnivore traces (pits, grooves, notches and gnaw marks) and digestion marks are present in 2% of bone remains and are principally associated with Units 2c and 4 (Fig. 5). A single coprolite measuring 32 mm^3 was recovered from the lowest part of Unit 2 d. Burning damage was also observed on 3.4% of remains, mainly from Units 2c and 3. Possible cutmarks were also identified on nine fragments of long bone recovered from Unit 2 d (a full summary of the macrofaunal taphonomic study is found in **supplementary information 2**).

Due to the high levels of fragmentation and taphonomic modification of the macrofaunal remains from Ararat-1, only 27 specimens could be taxonomically classified, representing seven species and 16 MNIs. The predominant taxa represented are middle-class sized caprines (*Capra ibex* and *Cabra* or *Ovis*), which occur in Units 2 b (1), 2 d (2), 3 (1) and 4 (6). Small carnivores include badger (*Meles meles*) recovered from Unit 2a, lynx (*Lynx* sp), recovered from Unit 4, and fox (*Vulpes vulpes*) recovered from Units 2a, 2 b and 2c. No large carnivore remains were identified in the sequence. Large ungulates are represented by a single tooth of *Equus* sp. recovered from Unit 4. A small number of lagomorph (NR = 4) and bird (NR = 4) remains were recovered from Units 2 d and 4 Units 2 b, 2 d and 3, respectively. A single refit on a dry bone fracture of a medium-sized ungulate radius found in Units 2a and 2c was also identified in the remains.

The microfaunal assemblage of Ararat-1 comprises 2437 bone remains. Almost half the remains were derived from Unit 2 b, whilst 20.7% of remains recovered from Unit 2a and 13.0% from Unit 2c. Microfauna counts for the rest of the sequence are relatively lower and account for 6.8% (Unit 2 d), 2.2% (Unit 3), 3.6% (Unit 4) and 1.1% (Unit 5). 1733 specimens (79% of total assemblage) were unidentifiable. Digestive modification is identifiable on almost all the remains (99.8%) and is mainly concentrated on the epiphyses and articular surfaces. Of these bones, 24.3% showed evidence of heavy and extreme digestion, whilst 39.7% and 35% showed evidence of moderate and light digestion, respectively.

Taxonomic classification of the microfaunal assemblage from Ararat-1 is shown in Table 6. The sequence is characterised by a wide range of mammalian and herpetofauna taxa. Small mammals include the Afghan pika (*Ochotona rufescens*), the southern white-breasted hedgehog (*Erinaceus concolor*) and the small five-toed jerboa (*Allactaga elater*). Single occurrences of Anatolian ground squirrel (*Spermophilus xanthoprymnus*), the European water vole (*Arvicola amphibius*), the common vole (Microtus arvalis), the bicolored shrew (*Crocidura leucodon*), the Levantine mole (*Talpa levantis*), and Nehring's blind mole rat (*Nannospalax xanthodont*) were also identified. Also evident are at least one species of the genus Meriones (possibly *Meriones dahli*) and remains from the subgenus Mus sp. The herpetofauna is represented by the variable green toad (*Pseudepidalea varibilis*), the Caucasian agama (*Paralaudakia caucasica*), the Levantine viper (*Macrovipera lebetina obtuse*), as well as multiple snake species of the family Colubridae.

Together, the macrofaunal and microfaunal remains from the Ararat-1 sequence allow for inferences to be made regarding the principal agents of accumulation and taphonomic alteration at the site. The presence of lynx and fox in the lower Ararat-1 strata (Units 2 d - 4) alongside coprolitic material and evidence of carnivore marks on bones suggests that carnivore activity was the principal agent of faunal accumulation in the lower part of the Ararat-1 sequence. Burnt bones and possible cutmarks on material derived from Units 2c and 2 d suggest that anthropogenic activity may have also contributed to the accumulation of faunal remains. The absence of these features in the upper Ararat-1 strata (Units 2a - 2 b), combined with a reduction in the volume of larger faunal material suggests a shift in the principal mode of accumulation. The presence of a high frequency of microfaunal remains, the majority of which have evidence of digestive modification, indicates that avian predation was driving bone accumulation at the site. The digestion patterns evident in the microfaunal assemblage are consistent with a large nocturnal avian predator, likely the Eurasian Eagle-owl (*Bubo bubo*; Andrews, 1990). Supporting this inference is the high

Table 5
Summary of macrofaunal remains from Ararat-1 cave. NISP (Number of Identified Species) of taxa, total undetermined and total number of remains (NR) for each stratigraphic unit.

Unit	Unit 2a	Unit 2 b	Unit 2c	Unit 2 d	Unit 3	Unit 4	Total	%
Taxon								
Equus sp.						1	1	**0.10%**
Capra/Ovis		1		1	1	6	9	**0.86%**
Capra ibex				1			1	**0.10%**
Lynx sp.						2	2	**0.19%**
Vulpes vulpes	1	2	1				4	**0.38%**
Melesmeles	2						2	**0.19%**
Lagomorph				3		1	4	**0.38%**
Bird		2		1	1		4	**0.38%**
Total NISP	**3**	**5**	**1**	**6**	**2**	**10**	**27**	**2.57%**
Total Undetermined	**34**	**31**	**96**	**292**	**252**	**318**	**1023**	**97.42%**
Total NR	**37**	**36**	**97**	**298**	**254**	**328**	**1050**	**100.00%**

diversity of faunal material that exhibits digestive modification, combined with the fact that this taxon has a wide Eurasian distribution, and a preference for rocky and mountainous areas with some woodland stands (Holt et al., 2013).

The Ararat-1 faunal assemblage provides compelling evidence of various taphonomic processes that have affected the remains. While there is limited evidence of weathering, the high degree of fragmentation and chemical alteration (dissolution and carbonate concentrations) of the bones suggests that post-depositional physiochemical alteration has occurred. The high fragmentation of bones is the result of a combination of breakage from high-energy sediment deposition within the cave and bioturbation of the sequence, primarily by root growth and faunal activity. This is supported by the presence of badger in the upper strata of the sequence and root moulds on many of the bone fragments, both of which strongly suggest that bioturbation of the upper strata has taken place. The percolation of calcium-rich vadose waters from the cave system through the Ararat-1 sequence is likely the primary cause of the observed chemical alteration of the surface of the bone remains.

Notwithstanding these taphonomic modifications, the faunal remains from Ararat-1 allow inferences to be made regarding prevailing environmental conditions at the time of sediment accumulation. Together, the presence of caprines (such as *Capra ibex)*, lynx and Equus sp suggest rocky and open environments. The occurrence of small mammalian taxa such as *O. rufescens, E. concolor, A. elater*, and *A. amphibius* indicates more of a mosaic landscape alternating between dry shrub and grassland and temperate woodland. Given the inferred predation of these small mammals was by the Eurasian Eagle-owl, then there was likely a water body within the hunting radius of this taxon (c. 40 km^2, Sándor and Ionescu, 2009; Amr et al., 2016, Guilland et al., 2018). The absence of small mammalian fauna commonly associated with humid conditions may also hint at relatively drier conditions at the Ararat-1 locale during the interval of accumulation.

4.4. Charcoal remains

212 charcoal fragments from Ararat-1 were analysed. The number of charcoal remains recovered from each stratigraphic unit is small, with half (n = 106) recovered from Unit 2c (Table 7). Biodegradation features caused by fungi and bacteria are evidenced in the charcoal remains with a small number of fragments also showing evidence of vitrification. Where possible, charcoal fragments were assigned a genus, family, or type-level classification. The most representative taxa in the Ararat-1 sequence is *Rhammus* sp., followed by Chenopodiaceae and *Prunus tp. Amygdalus*. The assemblage also yielded fragments belonging to Anacardiaceae, Asteraceae, Monocotyledoneae and *Tamarisk* sp. (Fig. 6).

The anthracological results from Ararat-1 should be interpreted cautiously given the low fragment numbers per stratigraphic level (Chabal, 1992). Broadly, the assemblage is characterised by the presence of semi-arid and arid taxa with low humidity requirements. Specifically, the presence of *Rhammus* sp. and Chenopodiaceae indicates open-shrub vegetation and dry conditions with a severe seasonal moisture deficiency. Evidence of vitrification (i.e., fusion of cellular tissue) may hint at the possibility of firewood acquisition strategies involving deadwood (e.g., Vidal-Matutano et al., 2017). However, the preliminary nature of the charcoal assemblage from Ararat-1 precludes a full interpretation of these findings.

4.5. Artefact assemblage

Two main artefact assemblages were recovered from the Ararat-1 sequence; a small ceramic assemblage recovered from the upper strata of the sequence (Units 1-2c), and a larger lithic assemblage recovered throughout the sequence.

The ceramic assemblages comprise a total of 55 fragments (supplementary information 3). 43 of these are attributed to the Chalcolithic period, 9 to the Late Bronze Age, and 3 to the Early Medieval Period. Many fragments represent body shards with a few that also preserve portions of vessel rims, necks, or bases. A third of the assemblage was found on the surface (n = 17), whilst the majority were found within Unit 2a (0.1–0.3 m below surface). 4, fragments, all attributed to the Chalcolithic period, were found in Unit 2 b (0.3–0.8 m below surface), whilst no fragments were recovered from below Unit 2 b.

The Ararat-1 lithic assemblage is comprised of 656 artefacts, of which 134 are smaller than 10 mm (Figs. 7 and 8). The majority of these were recovered from Units 2c (n = 265), 2 d (n = 151) and 2 b (n = 91), with only a small number of artefacts recovered from Units 2a, 3 and 4. The lithic assemblage is in mint condition with no macroscale evidence for secondary modification. Chert (n = 345), followed by obsidian (n = 282) are the dominant lithic raw materials, with single occurrences of dacite, chalcedony, mafic lava, sandstone and quartzite (Fig. 8). Chert is the most frequent raw material found in Unit 2c (n = 227), whilst obsidian is more frequent is all other units (n ranges from n = 2 to n = 85). Evident in the sequence is the size-partitioning of lithic remains. The obsidian component is comprised of a higher frequency of pieces

Table 6
Summary of microfaunal remains from Ararat-1 cave. NISP (Number of Identified Species) of taxa, total undetermined and total number of remains (NR) for each stratigraphic unit.

Unit	1	2a	2 b	2c	2 d	3	4	5	Total
Taxon									
Meriones sp.	1	15	4	0	3	5	14	0	**42**
Ochotona sp.	1	0	6	1	5	5	4	2	**24**
Spermophilus sp.	0	0	1	0	1	0	0	0	**2**
Nannospalax sp.	1	0	0	0	0	0	0	0	**1**
Mus sp.	0	0	1	0	0	0	0	0	**1**
Arvicola sp.	0	0	3	1	0	0	0	0	**4**
Cricetulus sp.	1	2	1	0	0	0	0	0	**4**
Allactaga sp.	1	2	2	0	0	0	0	0	**5**
Microtus sp.	0	7	10	1	0	0	0	0	**18**
Crocidura sp.	0	0	3	1	0	0	0	0	**4**
Talpa sp.	0	0	2	0	0	0	0	0	**2**
Erinaceus sp.	0	0	0	0	2	0	0	1	**3**
Serpentes	1	8	35	4	0	0	2	0	**50**
Anura	6	32	109	41	4	16	17	3	**228**
Lacertilia etc.	10	0	34	4	10	0	1	0	**59**
Urodela	0	3	2	1	0	0	0	0	**6**
Total undetermined	**79**	**383**	**836**	**231**	**123**	**23**	**40**	**18**	**1733**
NISP	**22**	**69**	**213**	**54**	**25**	**26**	**38**	**6**	**453**
Total	**101**	**452**	**1049**	**285**	**148**	**49**	**78**	**24**	**2186**
Percentage (%)	**4.6**	**20.7**	**48.0**	**13.0**	**6.8**	**2.2**	**3.6**	**1.1**	**100.0**

Table 7
Summary of Anthracological data from Ararat-1.

Unit	2a		2 b		2c		2 d	4		5
Taxa	n	%	n	%	n	%	n	n	%	n
Angiosperm	3		7	6.73	5	10.42				
Anacardiaceae			10	9.62	2	4.17				
cf Anacardiaceae					1	2.08				
Asteraceae	9	21.43	1	0.96	1	2.08				
Chenopodiaceae	9	21.43	12		16	33.33				
cf Chenopodiaceae	2	4.76			1	2.08				
Monocotyledoneae					1	2.08				
Prunus tp. *amygdalus*	1	2.38	10	9.62	5	10.42		1	4.35	
Rhamnus sp.	6	14.29	56	53.85	10	20.83	2	22	95.65	2
cf. *Rhamnus* sp.			6	5.77	3	6.25				
Tamarisk sp.			2	1.92						
Undetermined	1	2.38	2	1.92	3	6.25				
Total	31	100	106	100	48	100	2	23	100	2

<10 mm in comparison to the chert, with retouched pieces comprised of a high frequency of convergent scrapers (Fig. 7). The chert component is generally larger in size with representation of all stages of reduction sequence. Differences between the raw materials suggest that two modes of technological organisation may have operated at Ararat-1 cave. Whilst chert was principally transported onsite for initial reduction, the obsidian retouched pieces were likely transported to the cave where they were maintained, rejuvenated, and transported again.

The techno-typological affinities of the Ararat 1 lithic assemblages are shared with other late MP assemblages in the Armenian Highlands and southern Caucasus (Adler and Tushabramishvili, 2004; Adler et al., 2006; Moncel et al., 2015; Frahm et al., 2016; Glauberman et al., 2020a, b; Malinsky-Buller et al., 2021; Malinsky-Buller et al., 2021). Similar technological organisation related to the differences between local (chert) and far travelled (obsidian) raw material have also been identified in other MIS 3-aged sites in the region, including Ortvale Klde, Georgia (Adler et al., 2006; Adler and Tushabramishvili, 2004; Moncel et al., 2015), Kalavan 2 (Malinsky-Buller et al., 2021) and Yerevan cave (Gasparyan et al., 2014; Gasparyan and Glauberman, 2022; Yeritsyan, 1972; Yeritsyan and Semyonov, 1971).

5. Discussion

5.1. Ararat-1 site formation processes

Combined sedimentological, chronological, biological, and archaeological evidence from the Ararat-1 sequence provides evidence of site formation processes during the late Quaternary. Like other cave contexts (e.g., Farrand, 2001; O'Connor et al., 2017), there is evidence of post-depositional modification of the Ararat-1 sediments. This complicates the interpretation of the archaeological and environmental records derived from the sequence. The intrusion of Holocene material into the Pleistocene sediments, evident from the presence of pottery fragments and charcoal bearing a modern ^{14}C age, and bioturbation features within Units 1 and 2 b indicates disturbance of this part of sequence. However, the lower strata (Units 2c-5) remain relatively less disturbed. It may be that the rockfall event that resulted in the formation of Unit 2c may have sealed the lower strata, thus accounting for the reduced impact of recent anthropogenic and biological activity on these units and the archaeological and faunal material contained within. Translocation of fine-grained material within these underlying units is evident, leading to the modification of bone surfaces and a high number of unidentifiable remains. These translocation processes may have also contributed to the redistribution of finer material (e.g., charcoal) within the sequence. Whilst the current pIR225 age estimates cannot exclude the possibility of remobilisation of aeolian material, the coherence of the estimated ages through the sequence, and the agreement with ^{14}C ages in the lower strata suggest they provide a good estimate of the timing of sediment accumulation at this stage. Considering the uncertainties listed above, we can propose a model of changing principal agents of accumulation (geological, biological, and anthropogenic) through the Ararat-1 sequence that can be tested through further excavation and study.

The earliest sediment accumulation phase identified at Ararat-1 is documented in Units 5–3. The basal pIR225 measurement of the sequence indicates that sediment accumulation occurred by 52.4 ± 3.6 ka (Unit 4). The duration of this phase, estimated at 4–14 kyr, is supported by a sole ^{14}C age obtained from a charcoal fragment in Unit 3 (44,660–42,370 cal BP) and pIR225 ages from the same unit (44.3 ± 2.9 ka). Sedimentation during this interval was the result of a combination of aeolian processes and high-energy cave debris flows and collapse, as inferred from the bimodal size distribution of the cave sediments. The fragmented nature of the faunal material recovered from these units (and the entire Ararat-1 sequence) may be attributed to the periodic high-energy coarse-grained sedimentary inputs into the cave system, which could have caused bone material to break and crush. Despite these modifications, the faunal evidence from these units indicates that the cave was frequented by small carnivores during this period, supported by the presence of lynx remains, likely carnivore coprolitic material, and modification of bone fragments. The low lithic artefact density in these units suggests that the cave was only sporadically occupied by hominins during this time.

Although there is no clear evidence for significant changes in sediment deposition style, the archaeological and faunal material retrieved from Units 2 d-2b reveals a shift in the dominant agents of accumulation at Ararat-1 at around 45 ka (Unit 2 d: 45.1 ± 3.0 ka). The increased lithic artefact density found in these strata suggests that they represent the principal MP occupation phase within the cave. The pIR225 estimates from Unit 2 b (35.1 ± 2.5 ka) suggest that this period of occupation could have lasted for between approximately 5-10 kyr, but the indirect association of the luminescence and charcoal ^{14}C dates with human activity precludes a more precise estimate for the duration of hominin activity at the site until further chronological data is available. There is evidence of on-site core reduction of chert, retouching of obsidian raw materials and tools and potentially cut marked bone hinting at the ephemeral use of the site, possibly for processing meat. While there are indications of burnt bone and a rise in macrocharcoal remains in these layers, further anthracological data from the site is needed to evaluate the possibility of short-term, sporadic use of fire at this site. The faunal assemblage from these strata reveals a decrease in larger mammalian remains, as well as an increase in microfauna, indicating that the cave became predominantly a bird-nesting locale. The abundance of microscale phosphatic features in the sediments from these strata further suggests heightened faunal activity and associated excretory products. It is worth noting that ^{14}C ages derived from charcoal in Unit 2 b produced modern ages, indicating intrusion of modern material into these strata.

The third phase of sediment accumulation at Ararat-1 is

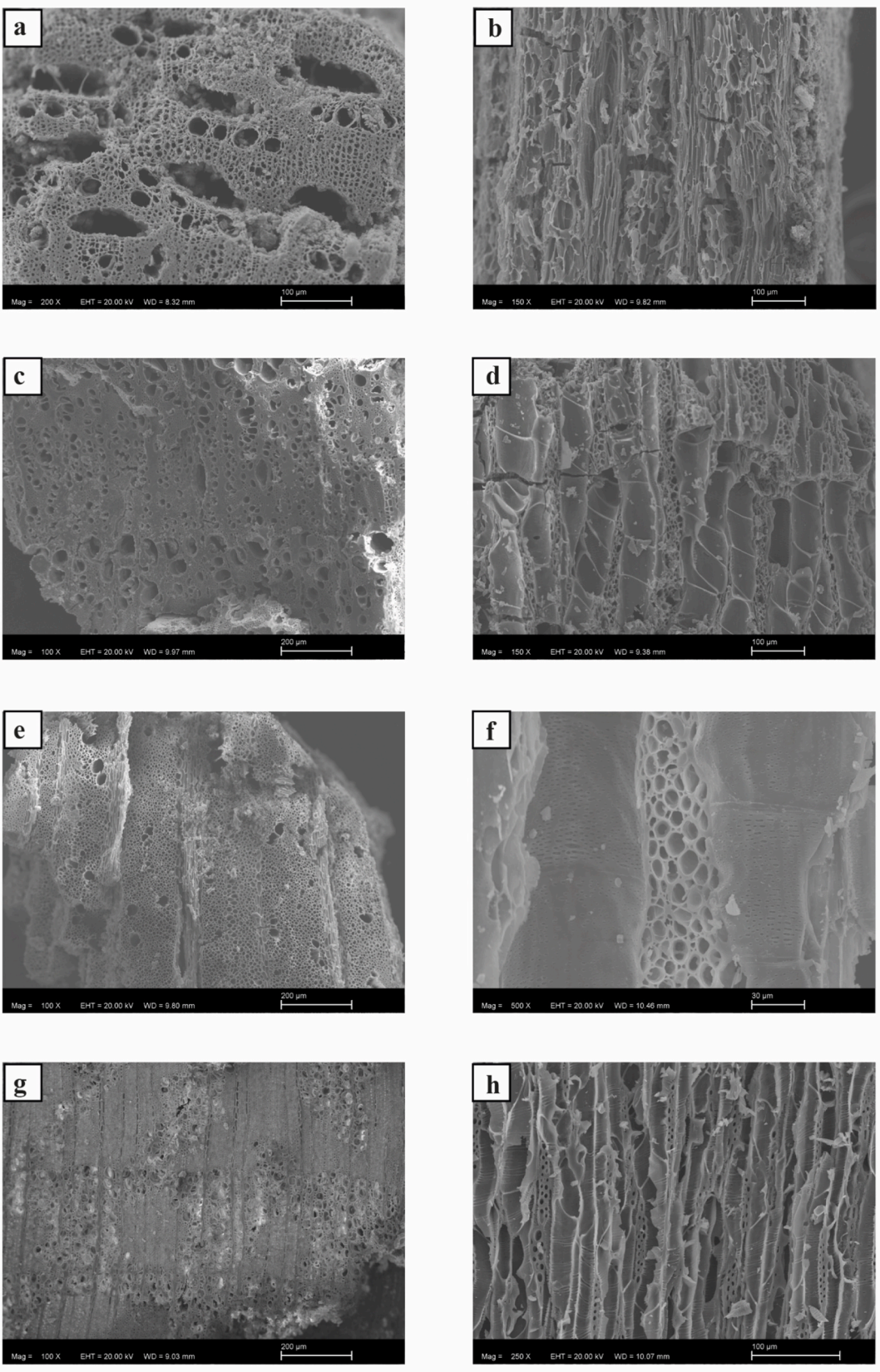

Fig. 6. SEM pictures of some of the woody taxa identified in Ararat-1. (A) Chenopodiaceae, transversal section (x200); (B): Chenopodiaceae, tangential section (x150). (C) Prunus tp. amygdalus, transversal section (x100). (D) Prunus tp. amygdalus, tangential section (x150). (E) Tamarix sp., transversal section (x100). (F) Tamarix sp., tangential section (x500); (G) Rhamnus sp., transversal section (x100). (H) Rhamnus sp., tangential section (x250).

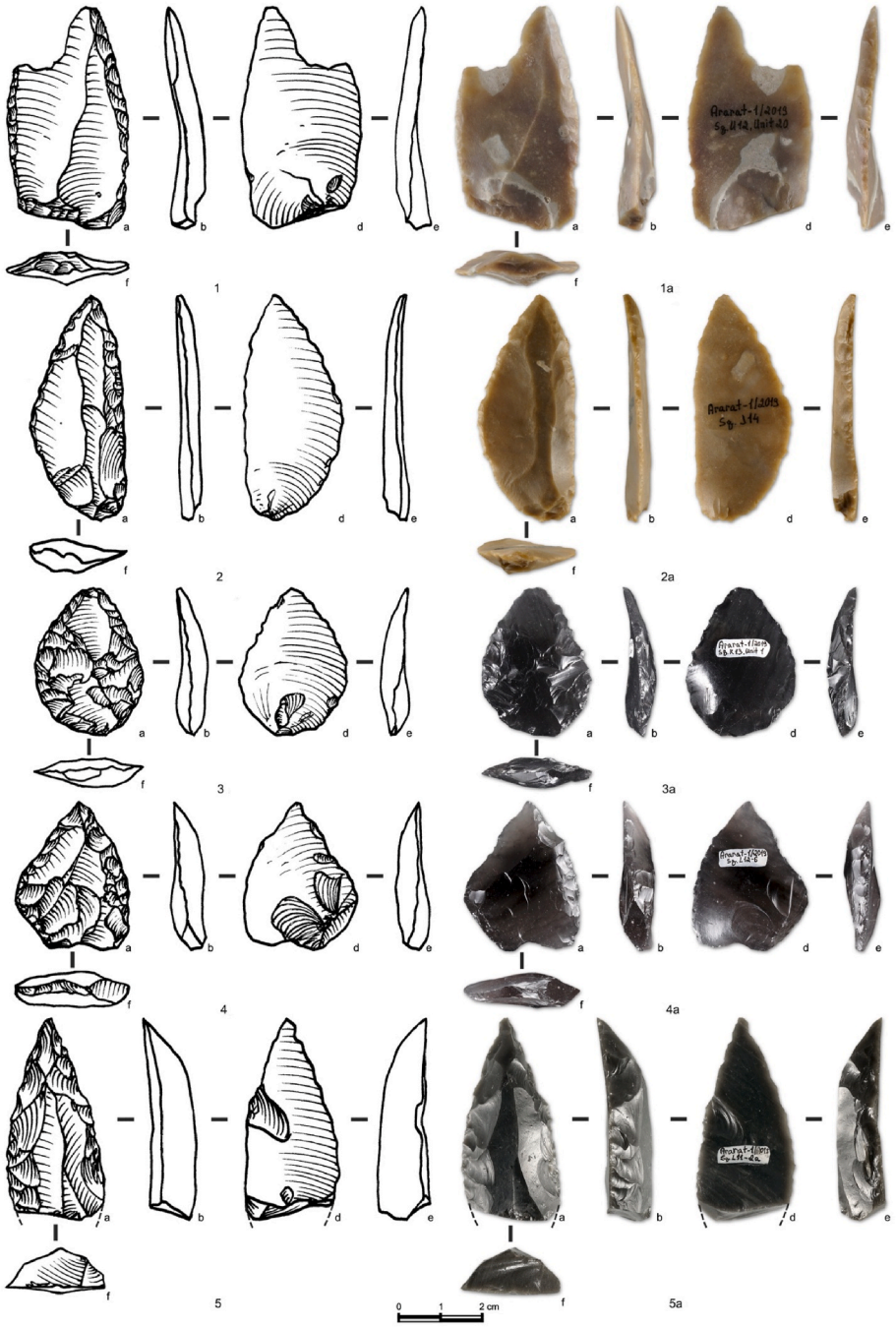

Fig. 7. Demonstrative lithic artefacts from Ararat-1. (1) Double side scraper made on chert (2) Double straight convex sidescraper made on chert. (3–5) Retouched points made on obsidian. More images can be found in supplementary information 3, Figs. S3–S5.

characterised by a decrease in lithic artefact densities and an increase in microfaunal remains within Unit 2a at 33.4 ± 2.5 ka. This indicates that the cave primarily served as a bird-nesting location and the main contributors to faunal accumulation were raptors, likely the Eurasian eagle owl. The presence of badger remains in this stratum may suggest that sediment mixing and burrowing could have occurred (Mallye, 2011; Arilla et al., 2020), which is supported by micromorphological evidence for faunal bioturbation. While low lithic artefact densities in this stratum may suggest sporadic hominin occupation, the age and stratigraphic integrity of these artefacts remains uncertain due to the small number of finds and evidence of mixing of more recent materials in this unit.

The most recent phase of sediment accumulation at Ararat-1 is represented by the presence of ceramic fragments from the Chalcolithic-Middle Age periods, which were found on the modern cave floor and in Unit 1. Modern organic material and excrement in Unit 1 indicate that the cave has been occupied recently. This recent anthropogenic and faunal activity has caused disturbance in the upper layers of the Ararat-1 sequence (Units 1a-2b), as indicated by the presence of ceramic fragments in these units, and by the modern ^{14}C ages of macroscale charcoal found in Units 2a-2b (cal AD 607–1634). Evident in the Ararat-1 sequence is a hiatus between the timing the latest interval sediment accumulation (at 33.4 ± 2.5 ka) and the accumulation of Holocene aged material within the older sediments. There are several probable explanations for this. First, this could be related to a reduction in cave sediment supply (i.e., a reduction in available fine-grained material for aeolian transport conditions), due to climate or broader landscape

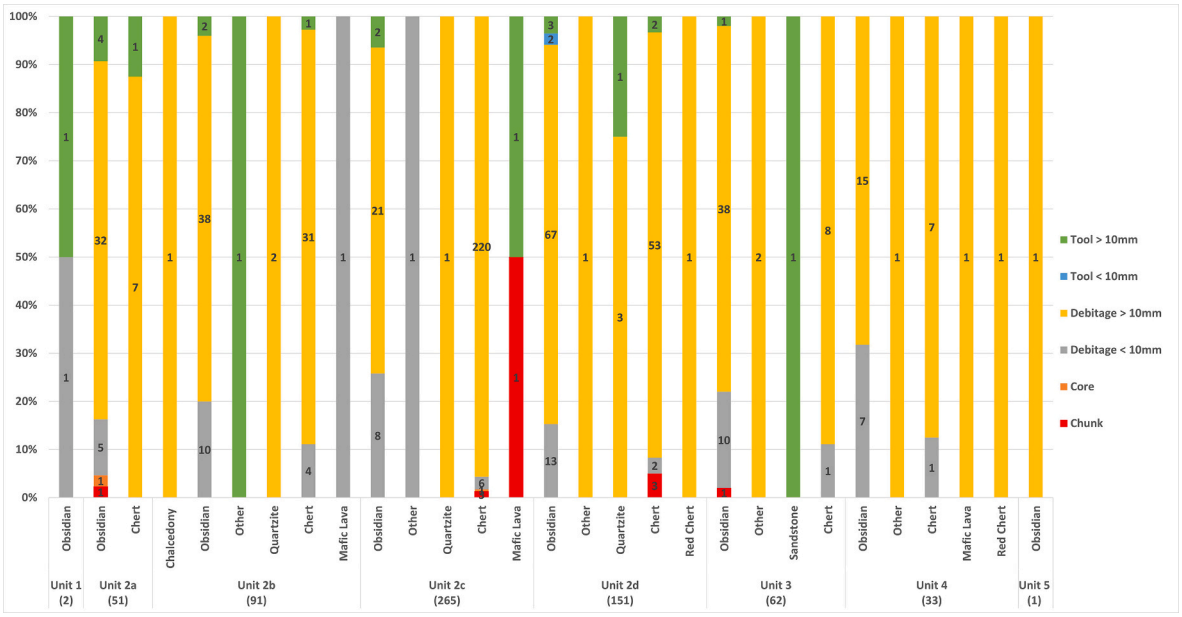

Fig. 8. Breakdown of Ararat-1 lithic artefact assemblage.

changes (e.g., Wolf et al., 2022). Second, the upper part the Ararat-1 sequence containing the MIS 2 and MIS 1 sediments may have been removed through erosion processes (i.e., a cave flood or deflation event). A third possible factor may be related to the sealing of the cave deposits or cave entrance due to colluvial processes, although there is no persuasive evidence for this in the vicinity of the cave entrance. Further excavation and chronological work at the site will help to ascertain the spatial distribution of the Ararat-1 deposits and elucidate the timing and the nature of this sedimentary hiatus.

5.2. Environmental and archaeological significance

The Ararat-1 sequence provides a depositional history spanning c. 52–35 ka. Despite the evidence of disturbance in the cave sequence, we currently consider this age to be accurate pending further chronometric study due to the homogeneity of ages from the two independent absolute dating techniques (pIR225 and ^{14}C) in Unit 2d. This date coincides with ages estimates of a range of late MP sites in the region, including Barozh-12 located on northern flanks of the Ararat Depression (Glauberman et al., 2020 a,b), Bagratashen-1 located in the Debed Basin (Egeland et al., 2016), and Kalavan-2 located in the northern flanks of the Areguni Mountains (Malinsky-Buller et al., 2021), and Lusakert-1 cave, located in the Hrazdan River valley (Sherriff et al., 2019).

Sedimentological and faunal evidence from Ararat-1 provides a record of environmental conditions during this occupation. The lack of substantial shifts in the style of sedimentation, combined with the absence of significant turnover in faunal populations suggests quiescent conditions around the cave locale during the interval of 52–35 ka. The presence of significant aeolian inputs into the cave is indicative of arid conditions that would have allowed for the mobilisation of fine-grained material from the Ararat Depression and the wider area into the cave. Together, the macro- and microfaunal remains indicate sediment accumulation under a semi-arid to arid climate regime during the MIS 3 period. The ecological niches, consisting of a mosaic of xerophytic open shrub, grassland, and temperate woodland around the cave locale, were like those found in the Ararat Depression today (Volodicheva, 2002). The prominent position of the cave, overlooking the low-lying palaeo-Araxes floodplain, together with these diverse ecological niches, would have been an appealing locale for MP occupation. Indeed, evidence for possible anthropogenic modification of bone material (cut-marks & burnt bone) may hint at the possibility that local fauna was used as a resource by hunter-gatherer populations.

The Ararat-1 lithic assemblage is comprised predominantly of chert and obsidian. Chert occurs locally in outcrops of Jurassic-Cretaceous ophiolites (Avagyan et al., 2018) around Vedi village, c. 10 km north of the cave. Alluvial fan deposits found on the western margin of the Ararat Depression close to the Ararat-1 cave entrance also contain chert (Karambagalidis, pers. observation), derived from the sedimentary and ophiolitic formations associated with the Urts Anticline. The prominent obsidian component in the Ararat-1 lithic assemblages indicates that obsidian was also exploited during the interval of cave occupation. The nearest obsidian sources are located at high elevations, including the Arteni volcanic complex on the western margins of the Basin (1754 m asl), Mt. Geghasar in the Gegham Highlands (2800–3100 m asl), and the Gutanasar volcanic complex in the Kotayk Plateau (1800 m asl), which lie 60–100 linear km away from Ararat-1. Although results of the chemical characterisation of the Ararat-1 obsidian artefacts are forthcoming, its presence in the Ararat-1 sequence indicates that these hunter-gatherer populations were able to access and use raw materials from a range of ecological niches along altitudinal gradients.

Ararat-1 contributes to the increasing number of MP sequences in the Armenian Highlands and southern Caucasus that allow for insights to be made regarding settlement organisation. Hunter-gather decision making relating to mobility has been suggested to be influenced by a range of ecological factors, including shifts in resource distribution and social demographic behaviours (Kelly, 2013). However, this is challenging to elucidate using lithic artefact characteristics (e.g., Bicho and Cascalheira, 2020) and/or faunal proxy evidence (Mitki et al., 2021). These challenges are further amplified when taking into consideration site formation processes and broader landscape-scale geomorphological agents. For example, differences in artefact densities at Ararat-1 (c. 30 n/m^3) and the nearby site of Barozh-12 (c. 1700–8000 n/m^3) may be interpreted in the context of behavioural variability, with apparent more frequent occupations at Barozh-12 a consequence of proximity to raw material and ecological resources (Glauberman et al., 2020a). However, the sediments at Barozh-12 have been subject to deflation processes, which may have acted to concentrate lithic material, resulting in these high densities. Similarly, taphonomic processes acting on the Ararat-1 sequence (sediment mixing, remobilisation and translocation) may have also acted to alter the relative density of lithic remains. Consequently, the use of artefact density as a behavioural marker should be used cautiously and site formation need to be taken into consideration in

Table 8
Summary of main sequences in the Armenian Highlands correlated to MIS 3 and their environmental infernces

Site	Elevation (m asl)	Age (ka)	Proxy evidence	MIS 3 Environmental Inferences	References
Ararat-1	1034	52–35	Sediments, macrofauna, microfauna, charcoal	Warm, semi-arid conditions	This study
Aghitu-3	1601	39-36 (layer AH VII); 36–32 (layer AH VI); 32–29 (layers AH V-IV)	Macrofauna, microfauna, botanical remains	Warm & humid climate (39–32 ka), cooling 32–39 ka	Kandel et al. (2017)
Barozh-12	1336	65–28	Sediments, biomarkers	Aridity (65–45 ka) followed by increased humidity (33–28 ka)	Glauberman et al. (2020a)
Hovk-1	2040	54.6 ± 5.7 (Unit 6); >46 (Unit 5)	Sediments, botanical remains, microfauna	Cold, dry & open conditions (55 ka) followed by more humid & vegetated conditions (33 ka)	Pinhasi et al., 2008, 2011
Kalavan-2	1640	60–45	Microfauna	Humid & relatively more vegetated	Malinsky-Buller et al. (2021)
Sevkar LPS	680	62-39 (pedocomplex L-1)	Sediments, Malacofauna	Arid conditions through MIS 3	Wolf et al., 2016, 2022; Trigui et al., 2019; Richter et al., 2020

these calculations (Bar-Yosef, 1998). Further work at Ararat-1 will focus on utilisation of the multiproxy evidence derived from the sedimentary sequence to achieve a better understanding of MP subsistence behaviours at the locale.

The evidence for stable conditions during MIS 3 at Ararat-1 may add to the growing body of evidence for localised differences in environmental conditions during this period (Table 8). For example, combined sedimentological and biomarker data from Barozh-12 indicates increased aridity from 65–45 ka, followed by a more humid phase from 33–28 ka (Glauberman et al., 2020a). Similarly, pollen and faunal evidence Hovk-1 suggest fluctuations between cold, dry, and open conditions around 55 ka, with more humid and vegetated conditions around 33 ka (Pinhasi et al., 2008, 2011). Conversely, the micro-faunal assemblage from Kalavan-2 indicates more humid and vegetated conditions during early MIS 3 (60–45 ka; Malinsky-Buller et al., 2021), whilst faunal remains from the Upper Palaeolithic site of Aghitu-3 suggest relatively warm and humid climate conditions similar to present-day from 39–32 ka, followed by cooling between 32 and 29 ka (Kandel et al., 2017). Although there is limited palaeoenvironmental evidence for MIS 3 elsewhere in the Armenian Highlands, malacological evidence from the loess-palaeosol sequences (LPS) in the Sevkar region shows a predominance of semi-desert and xerophilic steppe taxa, indicating persistently arid conditions throughout MIS 3 (Wolf et al., 2016, 2022; Trigui et al., 2019; Richter et al., 2020).

Whilst sites such as Barozh-12 align with regional palaeoclimatic records, the majority of data from the Armenian Highlands contrasts with the palaeoclimatic reconstructions from Lake Van during MIS 3, which exhibit fluctuations between relatively more arid and more humid conditions on a millennial scale (Litt et al., 2014; Stockhecke et al., 2016; Randlett et al., 2017). This divergence in local environmental conditions during MIS 3 could be due in part to site-specific preservation biases and chronological uncertainties, which limit direct correlation and comparison of environmental records. However, these differences may indicate local complexity in the expression of MIS 3 climates, with elevation being a contributing factor. Lower altitude sites, such as the Sevkar LPS (c. 680–980 m asl), Ararat-1, and Barozh-12, appear to record relatively more arid conditions during MIS 3 than sites located at higher altitudes, such as Hovk-1 cave and Kalavan-2. Evidence from the Sevkar LPS suggests that elevation amplified the effects of regional climate change over glacial-interglacial timescales. For instance, there is evidence for the contraction of forest communities into mid-altitude areas and the expansion of steppe communities into higher and lower-elevation areas during glacial/stadial periods due to enhanced aridity (Ritcher et al., 2020). This suggests that vegetation communities were shifting their altitudinal distribution in response to climate change. Although it is not possible to investigate these patterns within a single isotope stage such as MIS 3 at this time, it does suggest a close relationship between climatic variability, elevation, and ecological change in the Armenian Highlands. During MIS 3, local climatic variation would have resulted in a further diversity of ecological niches, providing MP populations with a wide resource base, potentially allowing them to persist in the Armenian Highlands much later than in other parts of Southwest Asia.

6. Conclusions

This study presents the first results of sedimentological chronological, faunal, and archaeological research on the MIS 3 cave sequence of Ararat-1, located on the eastern margins of Ararat Depression, Armenian Highlands. We demonstrated that sediment accumulation occurred between 52 and 35 ka and was caused by a combination of aeolian activity, cave rockfall and water action. Whilst the upper strata of the Ararat-1 sequence have undergone post-depositional disturbance due to faunal and anthropogenic processes, the cave sequence contains evidence for four phases of sediment accumulation during MIS 3 and the Holocene. Evident through the sequence are changing agents of accumulation, with the locale being used principally by carnivores, followed by more intensive hominin occupation and a subsequent interval on which the cave was principally used as a bird of prey locale.

During a stable period within MIS 3, Ararat-1 was inhabited by hominins amidst a mosaic of semi-arid shrub, grassland, and temperate woodland ecosystems. Hominins utilised both local and distant toolstone raw materials, suggesting they had the ability to adapt to a wide range of ecological and elevation gradients. Climatic reconstructions from Ararat-1 further highlight the spatial variability of MIS 3 environments and its role in hominin land use adaptations, demonstrating the importance of the Armenian Highlands for understanding regional MP settlement dynamics during a critical period of hominin dispersals and evolution.

Declaration of competing interest

The authors declare that they have no known competing financial interests or personal relationships that could have appeared to influence the work reported in this paper.

Data availability

Data will be made available on request.

Acknowledgements

This research was funded by The Gerda Henkel Stiftung grant (n. AZ 10_V_17 and n. AZ 23/F/19), the Fritz- Thyssen Foundation grant awarded for the project “Pleistocene Hunter-Gatherer Lifeways and Population Dynamics in the Ararat (paleo-lake) Depression, Armenia”, and The European Research Council grant N 948015: “Investigating Pleistocene population dynamics in the Southern Caucasus” (awarded to

AMB). Further support was provided by Gfoeller Renaissance Foundation (USA) and "Areni-1 Cave" Consortium ("Areni-1 Cave" Scientific-Research Foundation (Armenia) and the Institute of Archaeology and Ethnography of the National Academy of Sciences of the Republic of Armenia, the Gfoeller Renaissance Foundation, the Leakey Foundation and the Leverhulme Trust-funded Palaeolithic Archaeology, Geochronology, and Environments of the Southern Caucasus (PAGES) project (RPG-2016-102). We kindly thank the following individuals: Hovik Partevyan and the Partevyan Family, Suren Kesejyan, Pavel Avetisyan, Director of the Institute of Archaeology and Ethnography of the National Academy of Sciences of the Republic of Armenia, Paul Lincoln and George Biddulph.

Appendix A. Supplementary data

Supplementary data to this article can be found online at https://doi.org/10.1016/j.qsa.2023.100122.

References

Adler, D., Tushabramishvili, N., 2004. Middle Palaeolithic Patterns of Settlement and Subsistence in the Southern Caucasus.

Adler, D., BarOz, G., Belfer-Cohen, A., Bar-Yosef, O., 2006. Ahead of the game: middle and upper palaeolithic hunting behaviors in the southern Caucasus. Curr. Anthropol. 47 (1), 89–118.

Amr, Z.S., Handal, E.N., Bibi, F., Najajrah, M.H., Qumsiyeh, M.B., 2016. Change in diet of the eurasian eagle owl (Bubo bubo) suggests decline in biodiversity in wadi Al makhrour, bethlehem governorate, Palestinian territories. Slovak Raptor Journal 10, 75–79.

Andrews, P., 1990. *Owls, caves and fossils: predation, preservation and accumulation of small mammal bones in caves, with an analysis of the Pleistocene cave faunas from*. In: *Westbury-sub-Mendip*. University of Chicago Press, Somerset, UK.

Arilla, M., Rosell, J., Blasco, R., 2020. A neo-taphonomic approach to human campsites modified by carnivores. Sci. Rep. 10 (1), 6659.

Arutyunyan, E.V., Lebedev, V.A., Chernyshev, I.V., Sagatelyan, A.K., 2007. Geochronology of neogene-quaternary volcanism of the Geghama highland (lesser Caucasus, Armenia). Dokl. Earth Sci. 416 (No. 1), 1042. Springer Nature BV.

Avagyan, A., Sosson, M., Sahakyan, L., Sheremet, Y., Vardanyan, S., Martirosyan, M., Muller, C., 2018. Tectonic evolution of the northern margin of the cenozoic Ararat basin, lesser Caucasus, Armenia. J. Petrol. Geol. 41 (4), 495–511.

Badalyan, R., Harutyunyan, A., 2014. Aknashen–The Late Neolithic Settlement of the Ararat Valley: Main Results and Prospects for the Research. Stone Age of Armenia. A guide-book to the Stone Age archaeology in the Republic of Armenia, pp. 161–176.

Badino, F., Pini, R., Ravazzi, C., Margaritora, D., Arrighi, S., Bortolini, E., Figus, C., Giaccio, B., Lugli, F., Marciani, G., Monegato, G., 2020. An overview of Alpine and Mediterranean palaeogeography, terrestrial ecosystems, and climate history during MIS 3 with focus on the Middle to Upper Palaeolithic transition. Quat. Int. 551, 7–28.

Bailey, R.G., 1989. Bailey Ecoregions Map of the Continents. World Conservation Monitoring Center, Cambridge. https://www.unep-wcmc.org/resources-and-data/baileys-ecoregions-of-the-world.

Bar-Yosef, O., 1998. On the nature of transitions: the Middle to Upper Palaeolithic and the Neolithic Revolution. Cambridge Archaeological Journal 8 (2), 141–16.

Behrensmeyer, A.K., 1978. Taphonomic and ecologic information from bone weathering. Paleobiology 4 (2), 150–162.

Bicho, N., Cascalheira, J., 2020. Use of lithic assemblages for the definition of short-term occupations in hunter-gatherer prehistory. *Short-Term Occupations in Paleolithic Archaeology*. Definition and Interpretation 19–38.

Binford, L.R., 1981. Bones: Ancient Men and Modern Myths. Academic Press.

Blumenschine, R.J., Marean, C.W., Capaldo, S.D., 1996. Blind tests of inter-analyst correspondence and accuracy in the identification of cut marks, percussion marks, and carnivore tooth marks on bone surfaces. J. Archaeol. Sci. 23 (4), 493–507.

Bosch, R.F., White, W.B., 2004. Lithofacies and transport of clastic sediments in karstic aquifers. In: Studies of Cave Sediments: Physical and Chemical Records of Paleoclimate. Springer US, Boston, MA, pp. 1–22.

Bronk Ramsey, C., 2009. Bayesian analysis of radiocarbon dates. Radiocarbon 51, 337–360.

Bullock, P., Fedoroff, N., Jongerius, A., Stoops, G., Tursina, T., 1985. Handbook for Soil Thin Section Description. Waine Research.

Buylaert, J.P., Jain, M., Murray, A.S., Thomsen, K.J., Thiel, C., Sohbati, R., 2012. A robust feldspar luminescence dating method for Middle and Late P leistocene sediments. Boreas 41 (3), 435–451.

Chabal, L., 1992. La représentativité paléo-écologique des charbons de bois archéologiques issus du bois de feu. Bull. Soc. Bot. Fr. 139, 213–236.

Chu, W., McLin, S., Wöstehoff, L., Ciornei, A., Gennai, J., Marreiros, J., Doboș, A., 2022. Aurignacian dynamics in Southeastern Europe based on spatial analysis, sediment geochemistry, raw materials, lithic analysis, and use-wear from Românești-Dumbrăvița. Sci. Rep. 12 (1), 1–16.

Colonge, D., Jaubert, J., Nahapetyan, S., Ollivier, V., Arakelian, D., Devilder, G., Fourloubey, C., Jamois, M.-H., Gasparyan, B., Chataigner, C., 2013. Le Paléolithique Moyen de la haute valée du Kasakh (Arménie): caractérisation technologique et peuplement de montagne. Paleorient 39 (2), 109–140.

Dearing, J.A., 1999. Magnetic susceptibility. In: Walden, J., Oldfield, F., Smith, J. (Eds.), Environmental Magnetism; a Practical Guide. Quaternary Research Association Technical Guide No. 6, London.

Dee, M.W., Palstra, S.W.L., Aerts-Bijma, A.T., Bleeker, M.O., de Bruijn, S., Ghebru, F., Jansen, H.G., Kuitems, M., Paul, D., Richie, R.R., et al., 2020. Radiocarbon dating at groningen: new and updated chemical pretreatment procedures. Radiocarbon 62, 63–74.

Egeland, C.P., Gasparyan, B., Fadem, C.M., Nahapetyan, S., Arakelyan, D., Nicholson, C. M., 2016. Bagratashen 1, a stratified open-air Middle Paleolithic site in the Debed river valley of northeastern Armenia: a preliminary report. Archaeological Research in Asia 8, 1–20.

Fahn, A., Werker, E., Baas, P., 1986. Wood Anatomy and Identification of Trees and Shrubs from Israel and Adjacent Regions. Israel Academy of Sciences and Humanities.

Farrand, W.R., 2001. Sediments and stratigraphy in rockshelters and caves: a personal perspective on principles and pragmatics. Geoarchaeology: Int. J. 16 (5), 537–557.

Fernandez-Jalvo, Y., Andrews, P., 2016. Atlas of Taphonomic Identifications: 1001+ Images of Fossil and Recent Mammal Bone Modification. Springer.

Fewlass, H., Tuna, T., Fagault, Y., Hublin, J.J., Kromer, B., Bard, E., Talamo, S., 2019. Pretreatment and gaseous radiocarbon dating of40–100 mg archaeological bone. Sci. Rep. 9 (1), 5342.

Fewlass, H., Talamo, S., Wacker, L., Kromer, B., Tuna, T., Fagault, Y., Bard, E., McPherron, S.P., Aldeias, V., Maria, R., Martisius, N.L., 2020. A 14C chronology for the middle to upper palaeolithic transition at Bacho Kiro Cave, Bulgaria. Nature ecology & evolution 4 (6), 794–801.

Gasparyan, B., Glauberman, P., 2022. Beyond European boundaries: neanderthals in the Armenian Highlands and the Caucasus. In: Romagnoli, F., Rivals, F., Benazzi, S. (Eds.), Updating Neanderthals: Understanding Behavioral Complexity in the Late Middle Paleolithic. Academic Press, Elsevier, pp. 275–301.

Frahm, E., Feinberg, J.M., Schmidt-Magee, B.A., Wilkinson, K.N., Gasparyan, B., Yeritsyan, B., Adler, D.S., 2016. Middle Palaeolithic toolstone procurement behaviors at Lusakert cave 1, Hrazdan valley, Armenia. Journal of Human Evolution 91, 73–92.

Gasparyan, B., Egeland, C.P., Adler, D.S., Pinhasi, R., Glauberman, P., Haydosyan, H., 2014. The Middle Paleolithic occupation of Armenia: summarizing old and new data. In: Gasparyan, B., Arimura, M. (Eds.), Stone Age of Armenia. Center for Cultural Resource Studies, Kanazawa University, pp. 65–106.

Gevorgyan, H., Breitkreuz, C., Meliksetian, K., Israyelyan, A., Ghukasyan, Y., Pfänder, J. A., Sperner, B., Miggins, D.P., Koppers, A., 2020. Quaternary ring plain-and valley-confined pyroclastic deposits of Aragats stratovolcano (Lesser Caucasus): lithofacies, geochronology and eruption history. J. Volcanol. Geoth. Res. 401, 106928.

Glauberman, P., Gasparyan, B., Sherriff, J., Wilkinson, K., Li, B., Knul, M., Brittingham, A., Hren, M.T., Arakelyan, D., Nahapetyan, S., Raczynski-Henk, Y., 2020a. Barozh 12: formation processes of a late Middle Paleolithic open-air site in western Armenia. Quat. Sci. Rev. 236, 106276.

Glauberman, P., Gasparyan, B., Wilkinson, K., Frahm, E., Nahapetyan, S., Arakelyan, D., Raczynski-Henk, Y., Haydosyan, H., Adler, D.S., 2020b. Late Middle Paleolithic technological organization and behavior at the open-air site of Barozh 12 (Armenia). Journal of Paleolithic Archaeology 3, 1095–1148.

Goder-Goldberger, M., Crouvi, O., Caracuta, V., Horwitz, L.K., Neumann, F.H., Porat, N., Scott, L., Shavit, R., Jacoby-Glass, Y., Zilberman, T., Boaretto, E., 2020. The middle to upper paleolithic transition in the southern levant: new insights from the late middle paleolithic site of far'ah II, Israel. Quat. Sci. Rev. 237, 106304.

Golovanova, L.V., Doronichev, V.B., 2003. The middle paleolithic of the Caucasus. J. World PreHistory 17 (1), 71–140.

Guilland, E., Lebreton, L., Béarez, P., 2018. Taphonomic signature of Eurasian eagle owl (Bubo bubo) on fish remains. Journal of Vertebrate Biology 67, 143–153.

Hajdinjak, M., Mafessoni, F., Skov, L., Vernot, B., Hübner, A., Fu, Q., Essel, E., Nagel, S., Nickel, B., Richter, J., Moldovan, O.T., 2021. Initial upper palaeolithic humans in Europe had recent neanderthal ancestry. Nature 592 (7853), 253–257.

Heiri, O., Lotter, A.F., Lemcke, G., 2001. Loss on ignition as a method for estimating organic and carbonate content in sediments: reproducibility and comparability of results. J. Paleolimnol. 25 (1), 101–110.

Higham, T., Douka, K., Wood, R., Ramsey, C.B., Brock, F., Basell, L., Camps, M., Arrizabalaga, A., Baena, J., Barroso-Ruíz, C., Bergman, C., 2014. The timing and spatiotemporal patterning of Neanderthal disappearance. Nature 512 (7514), 306–309.

Holt, D.W., Berkley, R., Deppe, C., Enríquez Rocha, P., Petersen, J.L., Rangel Salazar, J. L., Segars, K.P., Wood, K.L., de Juana, E., 2013. Eurasian eagle-owl (Bubo bubo). In: Elliott, A., Sargatal, J., Christie, D.A., de Juana, E. (Eds.), Handbook of the Birds of the World Alive. del HoyoJ. Lynx Editions.

Hovers, E., 2009. The Lithic Assemblages of Qafzeh Cave. Oxford University Press.

Hovers, E., Belfer-Cohen, A., 2013. On variability and complexity: lessons from the Levantine Middle Paleolithic record. Curr. Anthropol. 54 (S8), S337–S357.

Hublin, J.-J., Sirakov, N., Aldeias, V., Bailey, S., Bard, E., Delvigne, V., Endarova, E., Fagault, Y., Fewlass, H., Hajdinjak, M., et al., 2020. Initial upper palaeolithic Homo sapiens from bacho kiro cave, Bulgaria. Nature 581, 299–302.

Inside Wood, 2004. InsideWood Database.

Kandel, A.W., Gasparyan, B., Allué, E., Bigga, G., Bruch, A.A., Cullen, V.L., Frahm, E., Ghukasyan, R., Gruwier, B., Jabbour, F., Miller, C.E., 2017. The earliest evidence for upper paleolithic occupation in the Armenian Highlands at aghitu-3 cave. J. Hum. Evol. 110, 37–68.

Karkanas, P., Goldberg, P., 2010. Site formation processes at Pinnacle point Cave 13B (Mossel Bay, Western Cape Province, South Africa): resolving stratigraphic and depositional complexities with micromorphology. J. Hum. Evol. 59 (3–4), 256–273.
Kelly, R.L., 2013. *The lifeways of hunter-gatherers: the foraging spectrum.* Cambridge University Press.
Lebedev, V.A., Chernyshev, I.V., Shatagin, K.N., Bubnov, S.N., Yakushev, A.I., 2013. The quaternary volcanic rocks of the Geghama highland, Lesser Caucasus, Armenia: geochronology, isotopic Sr-Nd characteristics, and origin. J. Volcanol. Seismol. 7, 204–229.
Lin, Y., Mu, G., Xu, L., Zhao, X., 2016. The origin of bimodal grain-size distribution for aeolian deposits. Aeolian research 20, 80–88.
Lisiecki, L.E., Raymo, M.E., 2005. A Pliocene-Pleistocene stack of 57 globally distributed benthic $\delta^{18}O$ records. Paleoceanography 20 (1).
Litt, T., Pickarski, N., Heumann, G., Stockhecke, M., Tzedakis, P.C., 2014. A 600,000 yearlong continental pollen record from Lake Van, eastern Anatolia (Turkey). Quat. Sci. Rev. 104, 30–41.
Lyman, R.L., 2008. Quantitative Paleozoology. Cambridge University Press.
Malinsky-Buller, A., Glauberman, P., Ollivier, V., Lauer, T., Timms, R., Frahm, E., Brittingham, A., Triller, B., Kindler, L., Knul, M.V., Krakovsky, M., 2021. Short-term occupations at high elevation during the middle paleolithic at kalavan 2 (republic of Armenia). PLoS One 16 (2), e0245700.
Mallol, C., Goldberg, P., 2017. Cave and rock shelter sediments. In: Nicosia, C., Stoops, G. (Eds.), Archaeological Soil and Sediment Micromorphology. Wiley Blackwell, Chichester, pp. 359–382.
Mallye, J.B., 2011. Badger (Meles meles) remains within caves as an analytical tool to test the integrity of stratified sites: the contribution of. Journal of Taphonomy 9 (1), 15–36.
Marín-Arroyo, A.B., Terlato, G., Vidal-Cordasco, M., Peresani, M., 2023. Subsistence of early anatomically modern humans in Europe as evidenced in the Protoaurignacian occupations of Fumane Cave, Italy. Sci. Rep. 13 (1), 3788.
Martirosyan-Olshansky, K., Areshian, G.E., Avetisyan, P.S., Hayrapetyan, A., 2013. Masis Blur: a Late Neolithic Settlement in the Plain of Ararat, Armenia. Backdirt, pp. 142–146, 2013.
Mellars, P., 2004. Neanderthals and the modern human colonization of Europe. Nature 432 (7016), 461–465.
Mitki, N., Yeshurun, R., Ekshtain, R., Malinsky-Buller, A., Hovers, E., 2021. A multi-proxy approach to Middle Paleolithic mobility: A case study from the open-air site of 'Ein Qashish (Israel). Journal of Archaeological Science: Reports 38, 103088.
Moncel, M.H., Pleurdeau, D., Pinhasi, R.O.N., Yeshurun, R., Agapishvili, T., Chevalier, T., Lebourdonnec, F.X., Poupeau, G., Nomade, S., Jennings, R., Higham, T., 2015. The Middle Palaeolithic record of Georgia: a synthesis of the technological, economic, and paleoanthropological aspects. Anthropologie 53 (1/2), 93–125.
O'Connor, S., Barham, A., Aplin, K., Maloney, T., 2017. Cave stratigraphies and cave breccias: implications for sediment accumulation and removal models and interpreting the record of human occupation. J. Archaeol. Sci. 77, 143–159.
Parsapajouh, D., Schweingruber, F.H., Lenz, O., 1987. Atlas of Northern Iranian Wood. University of Tehran Press.
Pederzani, S., Britton, K., Aldeias, V., Bourgon, N., Fewlass, H., Lauer, T., McPherron, S. P., Rezek, Z., Sirakov, N., Smith, G.M., Spasov, R., 2021. Subarctic climate for the earliest Homo sapiens in Europe. Sci. Adv. 7 (39), eabi4642.
Petrosyan, A., Arimura, M., Gasparyan, B., Nahapetyan, S., Chataigner, C., 2014. Early Holocene sites of the Republic of Armenia: questions of cultural distribution and chronology. Stone Age of Armenia 135–159. A Guidebook to the Stone Age Archaeology in the Republic of Armenia.
Pinhasi, R., Gasparyan, B., Wilkinson, K., Bailey, R., Bar-Oz, G., Bruch, A., Chataigner, C., Hoffmann, D., Hovsepyan, R., Nahapetyan, S., Pike, A.W.G., 2008. Hovk 1 and the middle and upper paleolithic of Armenia: a preliminary framework. J. Hum. Evol. 55 (5), 803–816.
Pinhasi, R., Gasparyan, B., Nahapetyan, S., Bar-Oz, G., Weissbrod, L., Bruch, A.A., Hovsepyan, R., Wilkinson, K., 2011. Middle Palaeolithic human occupation of the high-altitude region of Hovk-1, Armenia. Quat. Sci. Rev. 30 (27–28), 3846–3857.
Randlett, M.E., Bechtel, A., van der Meer, M.T., Peterse, F., Litt, T., Pickarski, N., Kwiecien, O., Stockhecke, M., Wehrli, B., Schubert, C.J., 2017. Biomarkers in Lake Van sediments reveal dry conditions in eastern A natolia during 110.000–10.000 years BP. G-cubed 18 (2), 571–583.
Rasmussen, S.O., Bigler, M., Blockley, S.P., Blunier, T., Buchardt, S.L., Clausen, H.B., Cvijanovic, I., Dahl-Jensen, D., Johnsen, S.J., Fischer, H., Gkinis, V., 2014. A stratigraphic framework for abrupt climatic changes during the Last Glacial period based on three synchronized Greenland ice-core records: refining and extending the INTIMATE event stratigraphy. Quat. Sci. Rev. 106, 14–28.
Reimer, P.J., Austin, W.E., Bard, E., Bayliss, A., Blackwell, P.G., Ramsey, C.B., Butzin, M., Cheng, H., Edwards, R.L., Friedrich, M., 2020. The IntCal20 Northern Hemisphere radiocarbon age calibration curve (0–55 cal kBP). Radiocarbon 62, 725–757.
Rentzel, P., Nicosia, C., Gebhardt, A., Brönnimann, D., Pümpin, C., Ismail-Meyer, K., 2017. Trampling, poaching and the effect of traffic. Archaeological soil and sediment micromorphology 281–297.
Richter, C., Wolf, D., Walther, F., Meng, S., Sahakyan, L., Hovakimyan, H., Wolpert, T., Fuchs, M., Faust, D., 2020. New insights into Southern Caucasian glacial–interglacial climate conditions inferred from Quaternary gastropod fauna. J. Quat. Sci. 35 (5), 634–649.
Sándor, A.D., Ionescu, D.T., 2009. Diet of the eagle owl (Bubo bubo) in Brasov, Romania. N. West. J. Zool. 5, 170–178.
Schweingrüber, F.H., 1976. Mikroskopische holzanatomic, Anatomie microscopique de bois. Institut féderal de recherches forestière, Zurcher AG.
Schweingrüber, F.H., 1990. Anatomie Europaischer Holzer: Anatomie of European Woods. Haupt, Stuttgart.
Shahack-Gross, R., Berna, F., Karkanas, P., Weiner, S., 2004. Bat guano and preservation of archaeological remains in cave sites. J. Archaeol. Sci. 31 (9), 1259–1272.
Sherriff, J.E., Wilkinson, K.N., Adler, D.S., Arakelyan, D., Beverly, E.J., Blockley, S.P.E., Gasparyan, B., Mark, D.F., Meliksetian, K., Nahapetyan, S., Preece, K.J., 2019. Pleistocene volcanism and the geomorphological record of the Hrazdan valley, central Armenia: linking landscape dynamics and the Palaeolithic record. Quat. Sci. Rev. 226, 105994.
Siddall, M., Rohling, E.J., Thompson, W.G., Waelbroeck, C., 2008. Marine isotope stage 3 sea level fluctuations: data synthesis and new outlook. Rev. Geophys. 46 (4).
Slimak, L., Zanolli, C., Higham, T., Frouin, M., Schwenninger, J.L., Arnold, L.J., Demuro, M., Douka, K., Mercier, N., Guérin, G., Valladas, H., 2022. Modern human incursion into Neanderthal territories 54,000 years ago at Mandrin, France. Sci. Adv. 8 (6), eabj9496.
Sosson, M., Rolland, Y., Müller, C., Danelian, T., Melkonyan, R., Kekelia, S., Adamia, S., Babazadeh, V., Kangarli, T., Avagyan, A., Galoyan, G., 2010. Subductions, obduction and collision in the Lesser Caucasus (Armenia, Azerbaijan, Georgia), new insights. Geological Society, London, Special Publications 340 (1), 329–352.
Stiner, M.C., Kuhn, S.L., Weiner, S., Bar-Yosef, O., 1995. Differential burning, recrystallization, and fragmentation of archaeological bone. J. Archaeol. Sci. 22 (2), 223–237.
Stockhecke, M., Timmermann, A., Kipfer, R., Haug, G.H., Kwiecien, O., Friedrich, T., Menviel, L., Litt, T., Pickarski, N., Anselmetti, F.S., 2016. Millennial to orbital-scale variations of drought intensity in the Eastern Mediterranean. Quat. Sci. Rev. 133, 77–95.
Stoops, G., Marcelino, V., Mees, F. (Eds.), 2018. Interpretation of Micromorphological Features of Soils and Regoliths. Elsevier. University of Chicago Press.
Talamo, S., Fewlass, H., Maria, R., Jaouen, K., 2021. "Here we go again": the inspection of collagen extraction protocols for 14C dating and palaeodietary analysis. Star: Science & Technology of Archaeological Research 7, 62–77.
Trigui, Y., Wolf, D., Sahakyan, L., Hovakimyan, H., Sahakyan, K., Zech, R., Fuchs, M., Wolpert, T., Zech, M., Faust, D., 2019. First calibration and application of leaf wax n-alkane biomarkers in loess-paleosol sequences and modern plants and soils in Armenia. Geosciences 9 (6), 263.
Yeritsyan, B.G., 1972. Nekotoriye ossobennosti namerennogo rassecheniya orudiy must'erskoy epokhi, po materialam Yerevanskoy peshchernoy stoyanki (Some features of intentional truncation of Mousterian tools, based on the materials of Yerevan cave site)I.T. In: Kruglikova (Ed.), soobshcheniya Instituta Arkheologii. Briefs of the Institute of Archaeology), N131, Kamenniy vek. Stone Age), Nauka, Moscow, pp. 53–60.
Yeritsyan, S.A., Semyonov, BG., 1971. Novaya nizhnepaleoliticheskaya peshchera Yerevan /New Lower Paleolithic cave of Yerevan. Kratkiye soobshcheniya. In: Instituta Arkheologii /Briefs of the Institute of Archaeology/, N126, Paleolit i Neolit /Paleolithic and Neolithic/. "Nauka" Publishing, Moskow.
van Klinken, G.J., 1999. Bone collagen quality indicators for palaeodietary and radiocarbon measurements. J. Archaeol. Sci. 26 (6), 687–695.
Van Meerbeeck, C.J., Renssen, H., Roche, D.M., Wohlfarth, B., Bohncke, S.J.P., Bos, J.A. A., Engels, S., Helmens, K.F., Sánchez-Goñi, M.F., Svensson, A., Vandenberghe, J., 2011. The nature of MIS 3 stadial–interstadial transitions in Europe: new insights from model–data comparisons. Quat. Sci. Rev. 30 (25–26), 3618–3637.
Vettese, D., Blasco, R., Cáceres, I., Gaudzinski-Windheuser, S., Moncel, M.H., Hohenstein, U.T., Daujeard, C., 2020. Towards an understanding of hominin marrow extraction strategies: a proposal for a percussion mark terminology. Archaeological and Anthropological Sciences 12 (2), 1–19.
Vidal-Matutano, P., Henry, A., Théry-Parisot, I., 2017. Dead wood gathering among Neanderthal groups: charcoal evidence from Abric del Pastor and El Salt (Eastern Iberia). J. Archaeol. Sci. 80, 109–121.
Volodicheva, N., 2002. The Caucasus. In: Shahgedanova, M. (Ed.), The Physical Geography of Northern Eurasia. Oxford University Press, New York, 350-37.
White, W.B., 2007. Cave sediments and paleoclimate. J. Cave Karst Stud. 69, 76–93.
Wolf, D., Baumgart, P., Meszner, S., Fülling, A., Haubold, F., Sahakyan, L., Meliksetian, K., Faust, D., 2016. Loess in Armenia–stratigraphic findings and palaeoenvironmental indications. Proc. Geologists' Assoc. 127 (1), 29–39.
Wolf, D., Lomax, J., Sahakyan, L., Hovakimyan, H., Profe, J., Schulte, P., von Suchodoletz, H., Richter, C., Hambach, U., Fuchs, M., Faust, D., 2022. Last glacial loess dynamics in the Southern Caucasus (NE-Armenia) and the phenomenon of missing loess deposition during MIS-2. Sci. Rep. 12 (1), 13269.